Design of Flight Test Systems for an Autonomous, Balloon-Launched Demonstrator for a Mars Exploration Airplane

by

Nelson A. Brown

B.A., University of Missouri Kansas City, Kansas City, Missouri 2001

Submitted to the Department of Aerospace Engineering and the
Faculty of the Graduate School of the University of Kansas
in partial fulfillment of the requirements for the degree of
Master of Science.

Dr. Richard Colgren (Committee Chairman)

Dr. David Downing (Committee Member)

Dr. Mark Ewing (Committee Member)

Dr. David Alexander (Committee Member)

Date defended: July 30, 2007

The thesis committee for Nelson A. Brown certifies that this is the approved version of the following thesis:

Design of Flight Test Systems for an Autonomous, Balloon-Launched Demonstrator for a Mars Exploration Airplane

Dr. Richard Colgren (Committee Chairman)

Dr. David Downing (Committee Member)

Dr. Mark Ewing (Committee Member)

Dr. David Alexander (Committee Member)

Date approved: _____

Abstract

Robotic airplanes have been proposed as a tool for surveying Mars. A Mars exploration airplane could bridge the scale and resolution gaps between orbiters and surface missions. Flight testing a prototype Mars airplane may be conducted at a very high altitude over the Earth, where the air density and temperature are representative of the conditions on Mars.

This research investigates the challenges of flight testing a Mars airplane prototype at high altitude and presents the design of a system and concept of operations that will deliver the required flight test data. The system transmits flight data to the ground via a wireless data link during the flight and records the data onboard the aircraft.

Subsystems that support the flight test system have been validated by tests on the ground and on high altitude balloons flights. Preliminary flight test data are presented to demonstrate the feasibility of this flight test operation.

Acknowledgements

I give thanks to Dr. Richard Colgren for his guidance and support during this research. I would also like to thank Dr. Mark Ewing and Dr. David Downing for their wisdom and advice. Many other people made significant contributions to this research including Dr. Subodh Bhandari and Dr. Shahriar Keshmiri whose knowledge and encouragement helped make this project successful. I would like to thank Mr. Wes Ellison and Mr. J. Andrew Pritchard for their help with electronic and mechanical issues. I especially would like to thank Dr. David Alexander for sharing his experience with electric model aircraft, helping to construct the low altitude test aircraft, and for piloting the aircraft during tests. The success of the high altitude balloon flights would not have been possible without the help of Dr. Trevor Sorensen, Mr. Steve Mance, Mr. Matt Brown, and the other members of the Experimental Balloon Society at the University of Kansas. I would like to thank Mr. Satish Chilakala for managing the avionics payload for one of the high altitude balloon flights. I would like to thank Mr. William Schweikhard for his advice and guidance. I appreciate the assistance Mr. Jim Rood gave me building the airplanes. Finally, I am deeply grateful for the loving support and encouragement from my wife, Sirikul Brown.

Table of Contents

List of Tables

List of Figures

Nomenclature

γ	Flight Path Angle
AAA	Advanced Aircraft Analysis (Software)
Alt	Altitude
c.g.	Center of Gravity
CF	Compact Flash
DATCOM	Data Compendium
DCM	Direction Cosine Matrix
ECEF	Earth Centered, Earth Fixed Coordinates
ENU	Local East, North, Up Coordinates
FAA	Federal Aviation Administration
g	Grams
G	Acceleration Due to Gravity on Earth, 9.80665 m/s^2 (32.174 ft/s^2)
GPS	Global Positioning System
HABS	High Altitude Balloon System
KU	University of Kansas
Lat	Latitude
Lon	Longitude
MATLAB	Matrix Laboratory (Software)
n	Load Factor
NASA	National Aeronautics and Space Administration
PWM	Pulse Width Modulation
r	Radius

SBC	Single Board Computer
UAV	Unmanned Aerial Vehicle
V	Velocity
w	Vertical Velocity
XBS	University of Kansas Experimental Balloon Society

1 Introduction

Among NASA's top goals is continued exploration of Mars. Some missions using robotic exploration by orbiter and ground rover have been successful. An airborne robotic explorer is being designed that would be able to survey large regions at higher resolution than rovers and orbiters (Levine, et al., 2003).

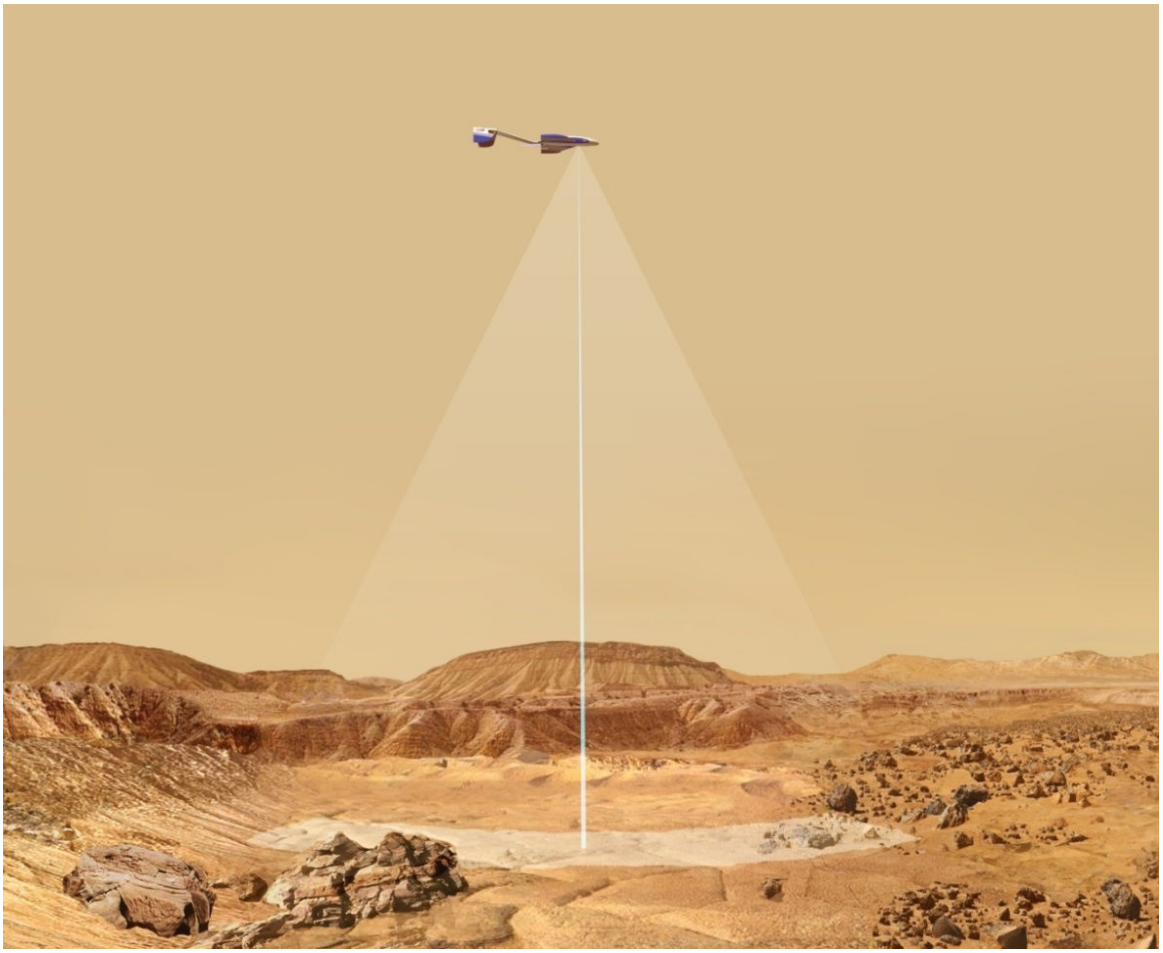

Figure 1-1: NASA Concept for a Mars Exploration Airplane

(ARES - A Proposed Mars Scout Mission, 2007)

Levine, et al., referring specifically to the ARES (Aerial Regional-scale Environmental

Survey of Mars) airplane design shown in Figure 1-1, say:

> ***ARES bridges the scale and resolution measurement gaps between the global-scale, lower resolution provided by orbiters and small-scale, higher spatial resolution provided by landers and rovers. Moreover, ARES can survey scientifically interesting terrain that is inaccessible to both landers and rovers. The three ARES scientific themes are: crustal magnetism, the underlying crustal mineralogy and geology and near-surface atmospheric chemistry.***

Other Mars airplane designs will seek to provide similar services to the scientific community. Flight testing a Mars airplane prototype requires special considerations because the Mars environment is so different from the Earth's.

Mars' atmosphere is thin compared to Earth's. The surface of Mars has large variations in elevation, from 8.2 km below to 21.2 km above the average radius of 3,396 km (Carr, 2007). The atmospheric pressure ranges from 0.7 mbar at the peak of Olympus Mons to 14 mbar at the deepest part of Hellas (Carr, 2007). The pressure also varies up to 25% depending on the season, as more of the atmosphere condenses during the longer, colder southern winter (Carr, 2007). At the landing site of Viking I the atmospheric pressure, about 7 mbar, is less than 1% of the Earth's atmosphere at sea level (Carr, 2007). However, at an altitude of about 34 km (110,000 ft) above the Earth, the air density is similar to that near the average surface of Mars (U.S. Standard Atmosphere, 1976). Designing an aircraft for this extreme environment is a challenge. Unconventional

design approaches and solutions are necessary for a successful mission.

Due to the low density of the Mars atmosphere, exploration aircraft will be designed for low Reynolds number flight more similar to birds and insects than to manned aircraft engineered for Earth. That is, for a Mars airplane the ratio of the inertia forces to viscous forces in the flow is similar to that of a bird. This ratio, called the Reynolds number, is "one of the most powerful parameters in fluid mechanics" (Anderson, Fundamentals of Aerodynamics, 2001). Just as dissimilar Reynolds numbers lead to scale effect problems between wind tunnel models and full size aircraft (Anderson, A History of Aerodynamics and Its Impact on Flying Machines, 1997), a Mars airplane designer can expect scale effect problems if flight testing of the Mars airplane is conducted at low-altitude on Earth. Many aircraft design tools have been developed based on successful aircraft for operation within the Earth's atmosphere (typically $Re \geq 10^7$); however, above Mars an airborne robotic explorer would encounter flow phenomena in the region of $Re \approx 10^4$. These flows are not as well-understood as those occurring at high Reynolds numbers. The performance of airfoils at low Reynolds numbers is poorly understood and generally results in unfavorable aerodynamics characteristics (Lee, Pang, Srigrarom, Wang, & Hsiao, 2006). Design and simulation tools for the low Reynolds number Martian environment would also be applicable to the development of Micro Aerial Vehicles (MAVs) for use on Earth.

Since a Mars airplane must be autonomous on its first flight on Mars, there is a need for a surrogate environment on Earth for flight testing. One method, used by NASA's ARES

(Aerial Regional-scale Environmental Survey of Mars) team and others, is to carry a prototype UAV to a high altitude above the Earth, approximately 34 km (110,000 ft), where the air density and temperature are representative of the flight conditions on Mars (ARES - A Proposed Mars Scout Mission, 2007). The ARES 50% scale model aircraft was lifted by a meteorological balloon. More information about the development of the ARES aircraft is described in the paper *Evolution of a Mars Airplane Concept for the ARES Mars Scout Mission* (Guynn, Croom, Smith, Parks, & Gelhausen, 2003).

Another important difference between the Mars and Earth environments is acceleration due to gravity; where Mars' gravity is roughly one-third of Earth's (Carr, 2007). The prototype Mars flyer will have no need for scientific payloads and therefore can be made less-massive than the actual Mars airplane it represents. Furthermore, the mass of additional batteries, fuel cells, or other energy sources should be greater on Mars in order to increase the endurance of the survey aircraft. Since the high altitude demonstrator aircraft can fly with less mass for a shorter demonstration flight, a total aircraft mass can be chosen that offsets the difference in gravitational acceleration so that the total force due to gravity acting on the airframe is similar to the actual Mars exploration aircraft. However, the flight test analysis will need to compensate for differences in inertia. While there is no suitable flight test region on Earth where the flight condition will exactly match that on Mars, high altitude flight testing is a valuable tool for validating a Mars airplane design.

A team of graduate students at the University of Kansas (KU) have designed a UAV for

the purpose of validating their design approaches through a series of flight tests. A rendering of the design is shown in Figure 1-2. After separating from the balloon, the aircraft conducts a pre-programmed series of maneuvers designed to investigate the dynamics of the aircraft.

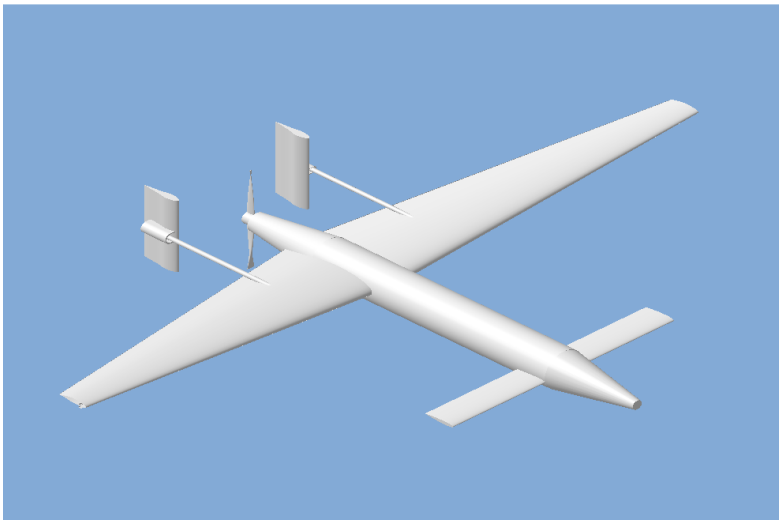

Figure 1-2: KU Mars Exploration Airplane Concept

Since the aircraft will be too far away to be seen, remote piloting would be difficult and would require a low-latency, high-bandwidth link. There would also be a significant risk of losing the link, even momentarily, that could cause the entire flight test to fail. Therefore, this aircraft will use an autonomous flight control system. This would be consistent with Mars operation.

The University of Kansas graduate student team developed the airframe design and a rough outline of the flight test. The design team produced drawings and analysis in a paper report. The author of this thesis started with that airframe design and continued

above and beyond with the development and implementation of the flight test system, a detailed method and process for flight testing, and data accumulated during the testing of the subsystems. The results of this research will aid the continued development of the Mars exploration airplane.

1.1 Problem Statement

The overall goal of the flight test system is to deliver high-quality data that demonstrates the dynamics of the subject aircraft. Since the data must be collected within low density air, the system must execute a complex process to reach high altitude, control the aircraft, and safely return the aircraft to the ground for recovery, as illustrated in Figure 1-3.

The flight test system is composed of several subsystems, including sensors, computers, digital radio modems, motor controller, control actuators, ground stations, and others. These subsystems also contain software onboard the aircraft and on the ground stations, for real time processing (flight management) and for analysis after the flight (post-processing). The flight management software is a combination of new customized code for this system and open source code available freely on the Internet (Jang, MNAV Autopilot, 2006). The post-processing software consists of original code interfaced with MATLAB and Simulink (MATLAB and Simulink, 1994-2007).

The cut-down from the lifting balloon must be triggered at the correct altitude. Since the release from the balloon may not occur immediately, the aircraft control system must be able to detect when the separation is complete.

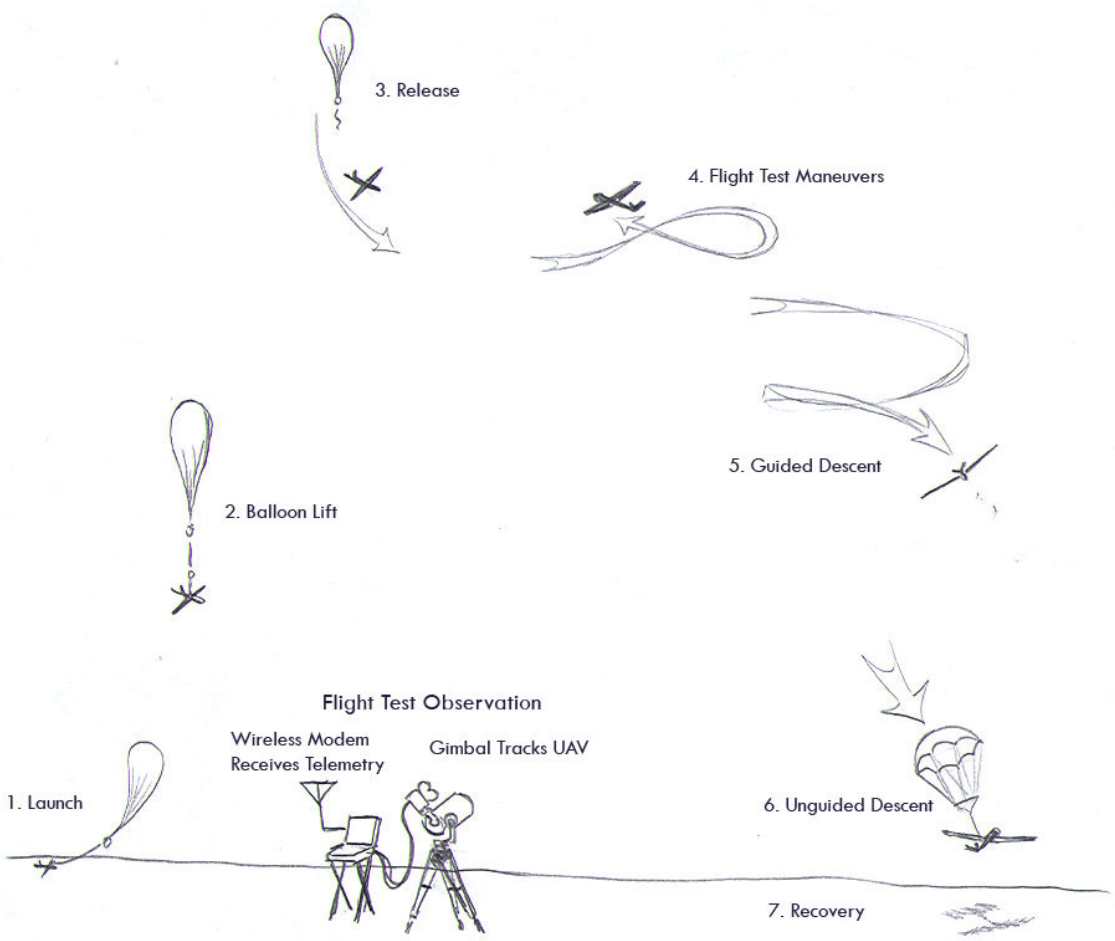

Figure 1-3: High Altitude Flight Test Summary

One method used to cut-down payloads from this type of balloon relies on a heated wire coiled around the cord connecting the payload to the balloon. When current is applied to the wire, the cord melts and breaks. The actual separation can lag a minute or more after the cut-down command is issued.

After separation from the balloon, the UAV will accelerate downward until the dynamic pressure is high enough to achieve adequate control authority. Immediately the aircraft

will begin to pull out of the dive, climb to reduce airspeed, and settle into steady level flight.

After the cruise trim condition is attained, the aircraft must execute doublets, frequency sweeps, and other open-loop maneuvers designed to excite the natural modes of the aircraft. Sensors must detect key vehicle states such as linear accelerations and rotational rates, which will be filtered to create an estimate of the position, velocity, and attitude of the aircraft during the maneuvers. Oscillations in the response to the doublet commands will demonstrate the natural frequencies and damping ratios or the major modes. These parameters will help refine the dynamic model of the aircraft and improve the analytical tools for predicting the dynamics of future Mars airplane designs.

During the flight test the sensor data will be recorded onboard the UAV on solid state media and also sent via radio link to one or more ground stations. The position, velocity, accelerations, angles, angular rates, air data, and control surface deflections will be communicated to the ground stations. The ground stations will display visualizations of the aircraft's trajectory and store the data for post processing after the flight test. The live data will be used to update predictions for the landing site so that the UAV can be recovered shortly after landing.

After the doublets and other demonstration maneuvers, the UAV will begin a gliding descent. A parachute will deploy and the UAV will gradually descend to the ground. The telemetry data must continue to stream to the ground stations all the way to the ground.

Analytical tools are used to predict the dynamics of the aircraft, and subsequently design a controller that maintains the desired trajectory and executes the required maneuvers. The controller must be implemented in software to be run on an embedded computer onboard the UAV.

Confidence in the flight test system will depend on evidence that the subsystems have sufficient performance to achieve the requirements for the mission. The subsystems must be tested to demonstrate performance in conditions similar to those expected during the high altitude flight test.

1.2 Research

The goal of this research is to integrate and implement the systems necessary to autonomously control a UAV for the purposes of flight testing. This includes gaining control of the aircraft after separation from a balloon, stabilizing flight to trim conditions, executing pre-programmed maneuvers such as doublets and frequency sweeps, transmitting flight data to the ground station, and safely recovering the aircraft.

The system consists of sensors, actuators, communications transceivers, embedded computers, and power supply. All of these components are inexpensive, commercial-off-the-shelf devices. The integrated airborne system is linked to two or more ground stations. Each ground station is independently capable of receiving and processing the telemetry data during the flight test.

During the development of the flight test system, various subsystems were validated with

ground tests and airborne tests. Three airborne tests were conducted. The first test demonstrated the functionality of the avionics and sensors at high altitude and proved that temperatures inside the avionics compartment could be maintained within the required range. The second test demonstrated the range and robustness of the communications system and utilized a mockup of the exterior shape of the aircraft to investigate the effects of gusts on the balloon, electronics modules, and aircraft prior to separation.

Figure 1-4: Low-Altitude Demonstrator Aircraft

The third airborne test utilized a hand-launched electric UAV, shown in Figure 1-4. This aircraft is a modified Bird of Time model sailplane. Among the modifications, an electric motor was added at the nose, and the wing was raised approximately 30 mm vertically to create additional payload volume near the c.g. (center of gravity). According to model airplane enthusiasts, the planform of this aircraft was inspired by the Thermic 100 free flight model airplane designed by Frank Zaic in 1940.

1.3 Results

The research discussed in this thesis resulted in knowledge and tools that will be useful for the continued development of a Mars exploration aircraft. The flight test system was flown to altitude to demonstrate that it provided reliable high altitude flight data acquisition. A long range telemetry system was set up, tested, and verified to provide communication over the distances required for the UAV flight test. The heat management system was confirmed to be sufficient for maintaining the temperatures required for the effective operation of the flight test system. A low altitude testbed aircraft was developed to support testing of various systems, including autopilots for autonomous flight. Through the implementation and testing of these systems, data sets were generated that will aid in the design revision of the high altitude UAV demonstrator.

2 Background and Related Projects

The design and testing of the high altitude flight test systems discussed in this thesis are related to other research work being done at the University of Kansas and at other institutions. Some of the most relevant related work is outlined here. Later sections make reference to these related projects.

2.1 KU Mars Airplane Design

As briefly referenced in the Introduction, during the fall semester of 2006 a team of graduate students at the University of Kansas, Department of Aerospace Engineering (KUAE) designed an aircraft for a regional survey of Mars. The author of this thesis was the chief engineer on this project. The design team partnered with Pittsburg State University to take advantage of their significant rapid-prototyping capabilities and with Kansas State University for their experience with embedded control systems. Also, the design team attained support from Eagle Picher in Joplin, Missouri and Lockheed Martin in Palmdale, California. With this wider team, a proposal was made in response to a NASA solicitation for state-wide aerospace design projects through the Kansas Space Grant Consortium (KSGC). The proposal won a NASA grant award, which made possible the acquisition of equipment for the construction of a high altitude UAV to demonstrate the Mars airplane design.

The final design, shown in Figure 2-1, would weigh about 44 N (10 lbs) on Earth. The total weight of the aircraft and the supporting balloon systems must not exceed Federal

Aviation Administration (FAA) regulated limits discussed in more detail on page 27. The Mars airplane conceptual design would have roughly triple the mass due to scientific instruments for survey and additional batteries for endurance, which leads to a similar weight on Mars. The design featured a variable incidence angle canard, and twin tail boom vertical tails. The tail booms connected to the release mechanism attached to the lifting balloon. The design team created a detailed report covering all aspects of the aircraft design, which is reference (Brown et al., 2006).

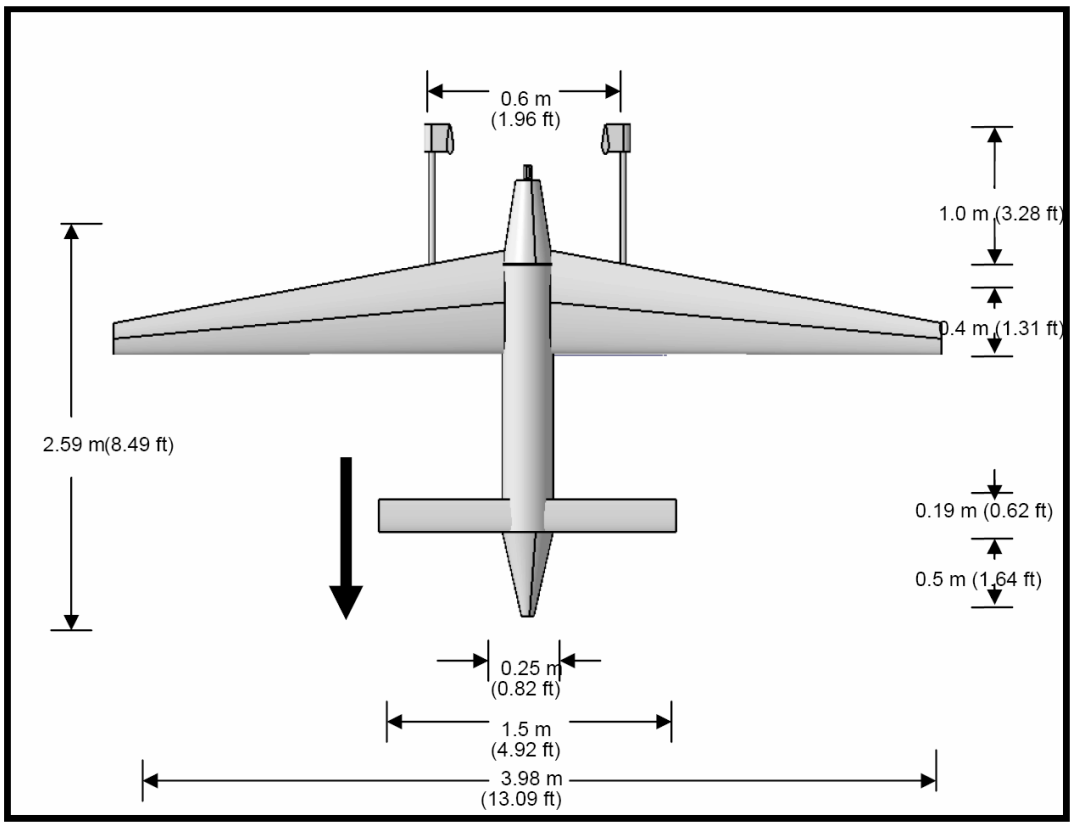

Figure 2-1: Mars Exploration UAV Demonstrator

During the design of the Mars aircraft and its Earth atmosphere high altitude demonstrator, many questions were raised about the feasibility of the flight test of the

aircraft. The team was uncertain that sufficiently lightweight batteries could provide enough energy for the entire flight test in the presence of very cold temperatures. While the advertized performance of radio modems indicated the flight test was feasible, the team was unable to test the range on the Earth's surface at representative ranges. During design reviews, the team learned of a phenomenon affecting electronics in very low density air called multipaction. It was unknown if this phenomenon would negatively affect the operation of the avionics at high altitude. Finally, besides a few rough simulations of the balloon drop, the design team had very little information about forward speed and load factors reached during the transition to normal flight. At the end of the semester, many of these questions were still unaddressed. This thesis picks up where the airplane design team finished. Multiple tests were conducted to address those questions. The results from these tests are discussed in Section 8. Also, the design team focused on the airframe and did not design the flight test procedure in detail. This thesis presents a detailed account of the flight test process, especially as it relates to the operation of the flight test systems.

2.2 High Altitude Flight Testing at NASA

A flight test program called APEX at NASA Dryden Flight Research Center aimed to lift a modified sailplane to high altitude to conduct low Reynolds number testing of airfoils. The NASA team concluded that the trajectory of the transition to normal flight was a risky component of the flight test (Lee, Bjarke, Greer, Tatineni, Zhong, & Jacobson, March 25-26, 1998). The NASA team considered the use of a drag parachute or a rocket to bring the aircraft into level flight after separation from the lifting balloon, as shown in

Figure 2-2. They found that without parachute or rocket assistance, the aircraft might accelerate in the dive to transonic speeds, or if the pull-out is too severe the load factor may exceed the limits of the structure.

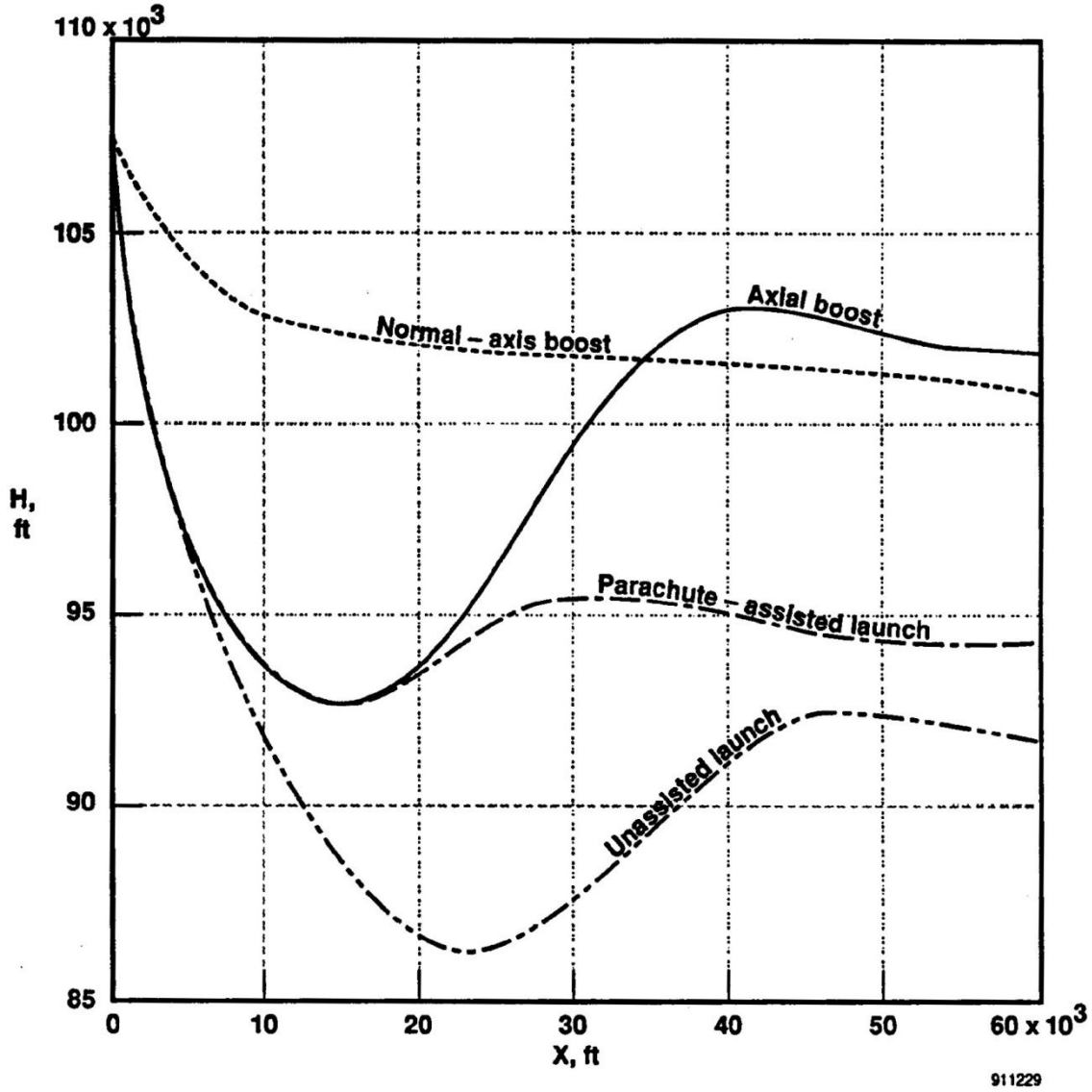

Figure 2-2: Predicted Trajectories for NASA's APEX Flight Test

(Murray et al., 1992)

High altitude, subsonic airplanes like the U-2, and likely Mars airplanes as well, run the

risk of entering a flight condition in the so-called "coffin corner." Due to the cold temperature, the speed of sound is slower. Meanwhile, due to the lower low Reynolds numbers airfoil performance is reduced and stall speeds are faster. The "coffin corner" exists where the stall speed gets close to the transonic range. In this condition, if the airplane pitches down slightly, it will speed up into the transonic range. This could be disastrous for aircraft with no wing sweep. On the other hand, if the airplane pitches up slightly, it will stall. The stall will cause it to pitch down, speed up, and again achieve transonic speed. A similar situation could cause problems for the propeller of the high altitude UAV, which is a realistic problem for the actual Mars airplane.

Some work has been done on low Reynolds number propeller design. Colozza designed a propeller for the APEX vehicle at NASA (Colozza, APEX 3D Propeller Test Preliminary Design, Sept. 2002). Colozza discusses the relevance to Mars airplane design and also presents the motor and battery design. Hall, Parks, and Morris have documented a detailed design of a propeller for a Mars airplane using optimization software (Hall, Parks, & Morris, 1997). Both reports state that very little data is available on this topic, and extensive testing is required. This is an interesting direction for wind tunnel research, which is discussed in Section 9.

2.3 UAV Flight Testing at KU

As part of the Center for the Remote Sensing of Ice Sheets (CReSIS) at the University of

Kansas, a team has designed a UAV for the survey of terrestrial ice sheets in Greenland and Antarctica using ground penetrating radar and other instruments. This UAV, called the Meridian, will use a commercial-off-the-shelf autopilot and satellite radio over-the-horizon communications for autonomous operations in polar regions. A rendering of the design is shown in Figure 2-3.

Figure 2-3: Meridian UAV for the Remote Sensing of Ice Sheets

The CReSIS team utilizes model aircraft kits, such as the scale model Yak-54 in Figure 2-4, in the development of the avionics system for the full size Meridian UAV. The

experiences from UAV flight testing for the CReSIS program have significantly influenced the design of the Mars airplane demonstrator flight test system and concept of operations.

Figure 2-4: Yak-54 Model as a Test Platform for UAV Avionics

2.4 High Altitude Balloon Operations

The High Altitude Balloon System (HABS) was developed by Nikhil Paruchuri at the University of Kansas as a master's thesis (Paruchuri, 2006). Figure 2-5 shows a balloon with the HABS slung below, just prior to launch.

This system is operated by the University of Kansas Experimental Balloon Society (XBS),

which is an extracurricular club that engages undergraduate and graduate students. Most of the participants are aerospace engineering or electrical engineering/computer science students. The balloon team lifts the HABS module and other payloads to high altitudes with meteorological balloons filled with helium.

Figure 2-5: High Altitude Balloon with Payloads

An example of a typical balloon flight profile is shown in Figure 2-6, copied from the *HABS-14 Flight Report* (Sorensen & Stiles, 2006). The summary of the HABS-14 flight

is quoted here, but the complete details are contained in *HABS-14 Flight Report* (Sorensen & Stiles, 2006). This particular flight on May 6, 2006 utilized a 1,500 g balloon, inflated to produce 70 N (16 lbs) of lift. The rate of ascent is nearly constant at about 6.8 m/s (1,330 ft/min), as the balloon expands from a diameter of about 2 m to more than 10 m, the buoyancy of the helium relative to the surrounding air remains the same.

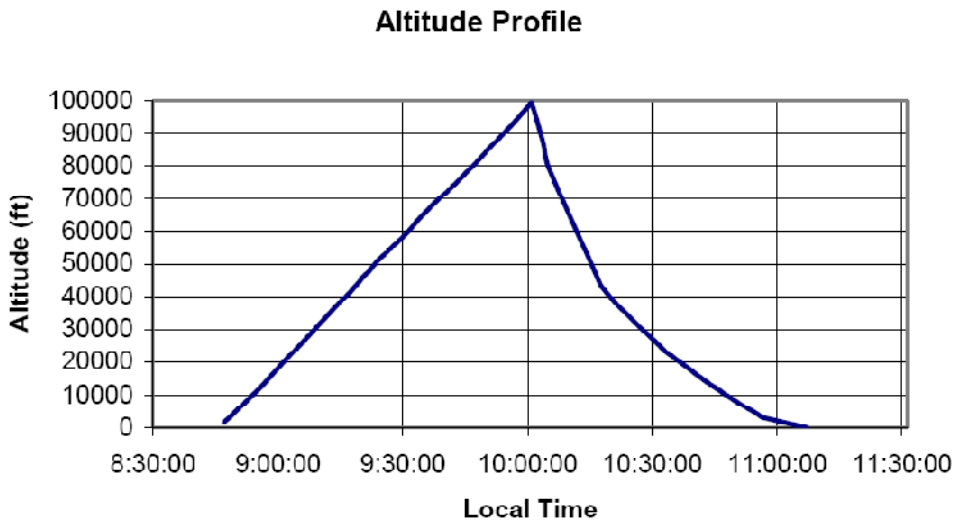

Figure 2-6: Typical Flight Profile of a High Altitude Balloon

(Sorensen & Stiles, 2006)

The highest recorded altitude was 30,268 m (99,304 ft). The ground crew issued a radio command to cut-down the HABS module from the balloon at 10:01 AM, and the module parachuted safely back to the Earth. The decent rate, dependent on the drag of the parachute, was initially fast and gradually slowed in the denser air at lower altitude. The average rate of decent rate was 7.5 m/s (1,485 ft/min).

3 Flight Test Plan

The design of the high altitude UAV flight test system includes complex systems that must be prepared and managed by a team of skilled individuals. The flight test plan describes the necessary coordinated actions of the UAV flight test team and their interaction with the XBS team. This flight test plan establishes a baseline for the operation of the flight test that defines requirements for all of the subsystems.

3.1 Concept of Operations

The flight test team will need a flight test engineer, an equipment engineer, and a safety officer. Two of these individuals will also be ground station operators during the flight test.

The University of Kansas Experimental Balloon Society (XBS) has been a valuable partner in the development of this high altitude flight test system. When the high altitude UAV final design is complete, the flight test team must coordinate with the XBS officers to facilitate the balloon launch and recovery of the UAV. XBS officers are familiar with the Federal Aviation Administration's regulations and procedures for unmanned free balloon operations. The balloon team has flown multiple flights with special FAA waivers to exceed the standard payload limitations. XBS has a good safety record and their reputation with the FAA is valuable to the completion of the high altitude flight test of a UAV.

For the high altitude UAV flight test, the flight test team must meet the requirements of

the XBS readiness reviews. At the Final Readiness Review (FRR), the XBS team will present the current weather forecast and the simulated trajectory of the balloon flight and payload recovery.

The team follows the balloon in chase vehicles. Usually the team uses two passenger vans rented from the University's Motor Pool. Vehicle Rental is a part of Facilities Operations at KU. Information is available online at http://www2.ku.edu/~kufo/. For the high altitude UAV flight test, an additional chase vehicle will be required to recover the UAV since it will land at a different location from the HABS. The Motor Pool requires the name of the department and the research grant, as vehicles are only available for official state business. The cost of renting a vehicle varies with fuel costs, and should be checked in advance of the flight test. The equipment engineer should reserve the vehicles a week in advance of the flight test. The drivers must be employees of the State of Kansas, such as graduate research assistants. Since the Motor Pool office is closed over the weekend, the equipment engineer will need to go to the Motor Pool office on Friday to complete the paperwork and pick up the keys. After the flight test, the keys and follow-up paperwork can be returned to a drop box at the Motor Pool.

Balloon flights are generally conducted on Saturday or Sunday mornings. The team prepares prior to the launch by charging batteries and sealing the payload containers. After the payloads are sealed, they are weighed. The balloon team calculated the required lifting force of the balloon to meet the required ascent rate. Typical ascent rates vary between 5 and 7 m/s (1,000 and 1,400 ft/min). The XBS payloads, such as HABS,

are sealed with silicone caulk to prevent water damage in the event the payload lands in water. Identification and contact information are clearly labeled on the outside of all payloads, as shown in Figure 3-1.

Figure 3-1: Balloon Payload Module External Label

Some payloads once thought lost have been returned to the team after other people discovered them. The balloon payload modules frequently land on private property, so clear markings are often important for recovery.

On the evening before the launch, the XBS radio technician will conduct tests of the

HABS telemetry and cut-down systems. If all the systems perform correctly, the launch is approved.

On the morning of the launch, the team meets at 5:00 AM to prepare the balloon, parachute, payloads, and chase vehicles. The equipment is moved from the lab to the launch site. The payloads are arranged vertically on a rack for the XBS team to string-through the cord that connects them. The high altitude UAV will be placed on a separate adjacent rack, so the aircraft can be connected to the cut-down mechanism below the HABS module. The XBS team unfolds the HABS parachute. The XBS team begins inflation of the balloon and checks the lifting force with a hand-held fish scale. The balloon team will calculate the correct lifting force required for the ascent.

The equipment engineer will prepare each chase vehicle prior to the launch. The XBS team will have a 144 MHz radio and laptop computer to record and display the telemetry data received from the HABS as well as aid in navigating rural highways. The UAV flight test team will supply two of the chase vehicles with a 900 MHz radio and an additional laptop to receive, record, and display the telemetry data from the UAV. XBS also equips the chase vehicles with power inverters connected to the vehicles' DC power. The inverter provides power to the radio modems and extends the operating time of the laptop computers. Most laptop computers currently available are not capable of operating for more than three hours on batteries, so external power is necessary to keep the computers running for the duration of the flight test. The equipment engineer should verify that the vehicle power supply is sufficient for the additional demands of the UAV

ground station computer and modem. The rugged laptops used for the UAV ground stations have longer battery life than standard laptops. Testing may reveal that vehicle power is not necessary for the rugged laptops. Each battery's performance will vary, and should be verified prior to the flight test.

Both the XBS team and UAV team will mount antennas on top of the chase vehicles. These antennas have magnetic mounts that attach to the roof of the vehicle. The antenna cables are usually fed through the left window of the van behind the driver's seat, because the right window is part of the sliding van door. The installation of the antennas and cables should be coordinated with the XBS team. During the chase of HABS-15, the 144 MHz radio's power cable was kicked loose, and several data packets were missed before the radio was back online. The antenna cables, power cables, and data cables should be carefully routed so they will not tangle in the crew's feet.

The XBS team has tray tables for laptops that attach to the rear of a van's front seats. Each chase vehicle will need a tray table for each laptop in that vehicle. The equipment engineer should coordinate with XBS to ensure that enough tray tables are available for the UAV flight test.

At least four team members are needed in each chase vehicle. Both ground station operators sit in the middle row of the van. One ground station operator will monitor HABS, while the other will monitor the UAV flight test. The ground station operators will provide information to the driver and the spotter. For the vast majority of the flight, the HABS and the UAV will be too high to be seen from the ground, and the ground

station operator will provide the navigation instructions to the driver based on telemetry data and updated software predictions of the landing site. When the HABS or UAV nears the ground at the end of the flight, the spotter will be looking skyward to see the parachute and will be giving instructions to the driver. However, for most of the chase, the spotter is responsible for operating the chase vehicle's GPS device, communicating with the base and other chase vehicles, and assisting the driver in spotting road signs, landmarks, and mile-markers.

The chase teams are likely to be driving for several hours in remote areas. Therefore, each team should prepare with plenty of drinking water, a first-aid kit, and other supplies. The high altitude UAV will likely use one or more lithium-ion or lithium-polymer batteries. If the landing causes a short circuit, these batteries have a risk of bursting and starting a fire. While the UAV will be designed to mitigate this risk, the chase team should be prepared with a fire extinguisher. Immediately after recovering the HABS or UAV, the team should turn off the system power with an external switch.

Since the HABS and UAV are likely to land on private property, the chase team should obtain permission to enter the property from the owners before attempting to recover the device. Entering private areas without permission may be considered trespassing, and could potentially be dangerous or unlawful. The chase teams should become familiar with the laws in both the states of Kansas and Missouri, as the jet stream tends to carry the balloon eastward.

The flight test team should also read and become familiar with FAA regulations. Within

the Code of Federal Regulations, Title 14: Aeronautics and Space, Part 101, Subparts A and D specifically relate to operations such as this balloon launch (GPO Access, 2007). Part 101 regulates the operation of moored balloons, kites, unmanned rockets, or unmanned free balloons. This flight test is designed to utilize an unmanned free balloon. Since the aircraft is the balloon's payload, an FAA waiver will be required to exceed the 6 lbs limitation (GPO Access, 2007). The UAV flight test is designed for winged flight only above 18,300 m (60,000 ft) altitude. The aircraft will deploy a parachute and descend to the ground just like the HABS and other high altitude balloon experimental payloads. FAA rules for visibility and radar reflectance should be observed in the design of the high altitude UAV in the parachute-descent configuration.

The usual cut-down mechanism used by the XBS team consists of a wire coiled around the cord connecting HABS to the balloon. When the radio command is received at HABS, a microcontroller switches on current to the wire coil. The coil heats up, and melts the cord. The cut-down is not immediate, and the delay between the issuance of the command and the drop of HABS is unpredictable. As an alternative or backup, the UAV could make use of special servos. Remote control aircraft hobbyists often actuate retractable landing gear with special servos that turn 180 deg. The Futaba S136G and Hitec HS-75BB are two examples of retract servos. These are "bang-bang" actuators that may only be commanded to full-up or full-down positions unlike typical proportional servos. The advantage of a retract servo in this application is that energy consumption in the held position should be considerably less than a proportional servo. The capability of a retract servo to hold position without drawing current was reported by RC hobbyists,

but could not be confirmed or denied based on manufacturer documentation or other published sources. The UAV team should test retract servos for torque, rise time, and energy usage.

Retract servos may also perform well for other tasks during the flight test. A retract servo may be a good choice as a primary or secondary method for triggering the deployment of the parachute after the UAV descends to about 18,300 m (60,000 ft). Also, an alternative concept for the transition from the balloon drop to normal flight calls for the UAV to enter and recover from a controlled deep stall. It is proposed here that a proportional servo be combined with a retract servo using a mechanical mixer mechanism to allow the stabilator to reach large negative incidence angles during the deep stall and return to normal incidence angles for normal flight. Research into controlled deep stall flight is discussed on page 44. Details about the implementation of the retract servo are discussed on page 47.

Each of the participants in the flight test will follow detailed steps described in the flight test "dance cards." These cards provide a common procedure to improve safety and help ensure that useful data is gathered during the flight test. Table 3-1 summarizes the dance cards for the high-altitude flight test of the Mars UAV demonstrator. The complete set of flight test dance cards is contained in Appendix B.

Table 3-1: Flight Test Dance Cards Summary

Card Number	Test Phase	Description
1	Prelim	Line-Up
2	Prelim	Mission Limits
3	Prelim	Preflight Tests
4	Ascent	Balloon Prep / Chase 1
5	Ascent	Balloon Launch
6	Ascent	Chase 2 / 3
7	Cut-Down	Drop / Pull-Up
8	Test Maneuvers	Test Maneuvers
9	Descent	Begin Descent
10	Descent	Parachute Deploy
11	Recovery	Track / Recover

3.2 Subsystems Tests

The complete flight test system depends on the successful implementation of several interdependent subsystems. In order to build confidence in the design of these subsystems, a series of specific tests were designed to be conducted on the ground and at high altitude. The high altitude tests were added as supplemental payloads on the HABS-15 and HABS-16b balloon flights. These tests are discussed in detail in the Flight Tests chapter beginning on page 74. The XBS account of the HABS-15 flight is described in the *HABS-15 Flight Report* (Sorensen & Stiles, 2007).

3.3 Flight Test System Requirements

The flight test must ultimately deliver high quality data that validates the aircraft design. All of the components of the flight test system contribute in some way to the safe operation of the aircraft or the collection and storage of the flight data.

The aircraft must ascend to high altitude where the flight conditions are representative of Martian conditions. The altitude must be approximately 33,000 m (110,000 ft) after the aircraft transitions to level flight.

The aircraft must fly under power long enough to execute the open-loop maneuvers and stabilize between them. This required endurance determines the size of the battery for the motor. The battery must be kept warm in order to maintain performance.

The UAV must be fully autonomous from the balloon launch to the parachute landing. Therefore, the avionics must have power for up to four hours of flight time.

The flight test system must have a wireless communications system that transmits all of the pertinent flight data from the UAV to the ground stations throughout the balloon ascent, flight test maneuvers, and descent. The experience of the XBS team shows that a typical balloon payload may land up to 142 km (88 mi) from the launch site (Sorensen & Stiles, HABS-14 Flight Report, 2006), (Sorensen & Stiles, HABS-15 Flight Report, 2007), (Paruchuri, 2006). Similar ranges have also been documented by the Edge of Space Society (Glahn, 2007). However, the first XBS chase vehicle leaves the launch site before the balloon begins its ascent, and the chase vehicle generally keeps a lateral

separation of less than 54 km (34 mi) from the balloon. Considering the vertical separation increases to an apex of about 35 km (22 mi), the worst-case hypotenuse is estimated to be 64 km (40 mi), ignoring the curvature of the Earth. Therefore, the radio modems are required to have a line-of-sight range of over 64 km (40 mi). It is also important that the chase vehicle receiver be near the landing site as the UAV descends to a low altitude, as the line-of-sight will become obfuscated by trees, buildings, and terrain.

The data stream must have bandwidth allowing for two 32-bit channels for latitude and longitude, and fourteen 16-bit channels for states at a sample rate of 50 Hz. This stream totals 14.4 kbps, but additional allowance must be made for error-correction overhead.

The high altitude UAV's autopilot must control the transition from the balloon drop to steady, level flight, execute doublet maneuvers to excite the natural modes of the aircraft, and glide the aircraft down to 18,300 m (60,000 ft) where the recovery parachute is deployed.

The recovery parachute must have two independent mechanisms that trigger its release. The primary trigger should be based on the autopilot's estimation of the aircraft's altitude, which is based on GPS and inertial sensors. The secondary trigger should be based on a separate altimeter switch. A system fitting these criteria was designed by the graduate student team at the University of Kansas (Brown et al., 2006).

4 Model Development

The success of the high altitude UAV flight test will depend upon the successful development and implementation of an autonomous control system. The design of the control system begins with a mathematical model of the forces and moments acting on the aircraft. A complete dynamic model of the aircraft for the entire flight envelope would be complex, but by focusing on a specific flight condition and assuming a number of simplifications, separate individual models can be used to evaluate certain key periods of the aircraft's mission.

The method proposed here is an iterative process. First, a reasonable trajectory is estimated. Second, the aerodynamic coefficients and derivatives are estimated with methods similar to DARcorporation's Advanced Aircraft Analysis (AAA) software or the USAF Stability and Control DATCOM (Data Compendium) for several points along the predicted trajectory. These parameters are suited to a linear model that is only valid for a small region around trim at that specific point on the trajectory. For the initial pull-out after the UAV is cut down from the balloon, a constant pull-up maneuver should be assumed. That is, the pitch rate q should be positive and constant. Third, using classical root-locus methods, a simple controller is designed with a gain schedule matching the time of the predicted trajectory. Fourth, a numerical simulation is run using a Simulink model that uses table look-up routine to find the scheduled gains. Finally, the trajectory is revised whenever it varies from the simulation by a significant amount. The allowable variation from the prediction is dictated by the validity of the linearized model at that

point. Many of the coefficients and derivatives relevant to the UAV's transition from nose-dive to level flight vary significantly as functions of angle-of-attack and Mach number. These steps must be repeated until the simulated trajectory closely matches the points used for linearization.

The first controller to be developed will be for a low-altitude UAV that will demonstrate the autonomous launch from a balloon, pull-out, flight test maneuvers, and parachute recovery. The model development process for this low-altitude aircraft is similar to the process that will be used on the high altitude Mars airplane demonstrator. Basic parameters for the low-altitude demonstrator are given in Table 4-1.

Table 4-1: Properties of the Low-Altitude Demonstrator Aircraft

Property	Symbol	Value	Units
Mass	m	1.51	kg
Wing Reference Area	S	0.67	m^2
Stabilizer Reference Area	S_h	0.10	m^2
Longitudinal Reference Length (chord)	$\bar{c}$	0.20	m
Lateral Reference Length (span)	b	3.00	m

The low-altitude demonstrator uses an Eppler 205 airfoil for the wings. The contour of this airfoil is shown in Figure 4-1. This airfoil is very similar to the Eppler airfoils used by the Rascal 110 UAV described by Jodeh, Blue, and Waldron (Jodeh, Blue, & Waldron, 2006). Reference (Jodeh, Blue, & Waldron, 2006) contains additional information about

the performance of this airfoil at low Reynolds numbers, as well as flight test data.

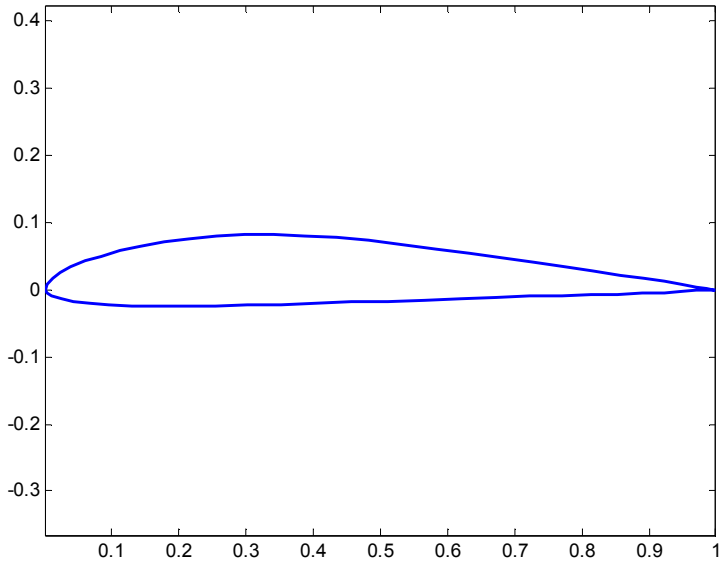

Figure 4-1: E205 Airfoil Contour

A similar Eppler airfoil, E387, was wind tunnel tested at low Reynolds numbers at NASA Langley Research Center in research related to the ARES Mars airplane (Re, Odis C. Pendergraft, & Campbell, 2006). Re et al. tested several additional candidate airfoils in a variety of configurations. Data from these wind tunnel tests should be useful to designers of Mars airplanes and their control systems.

4.1 Measuring Moments of Inertia

The mass polar moments of inertia of the aircraft will be measured with a simple three-string torsional pendulum, using the method described by Wagner and Cooney (Wagner & Cooney, 1979). The aircraft is placed on a triangular platform suspended by three cables, each equally spaced from the center of the platform. In Figure 4-2, foam blocks

are used to cradle the aircraft vertically so that the c.g. is directly above the center of the platform and the x-axis is plumb. The period of oscillation is measured by timing 50 cycles. The process should be repeated until three consecutive trials result in similar times, within a small percentage.

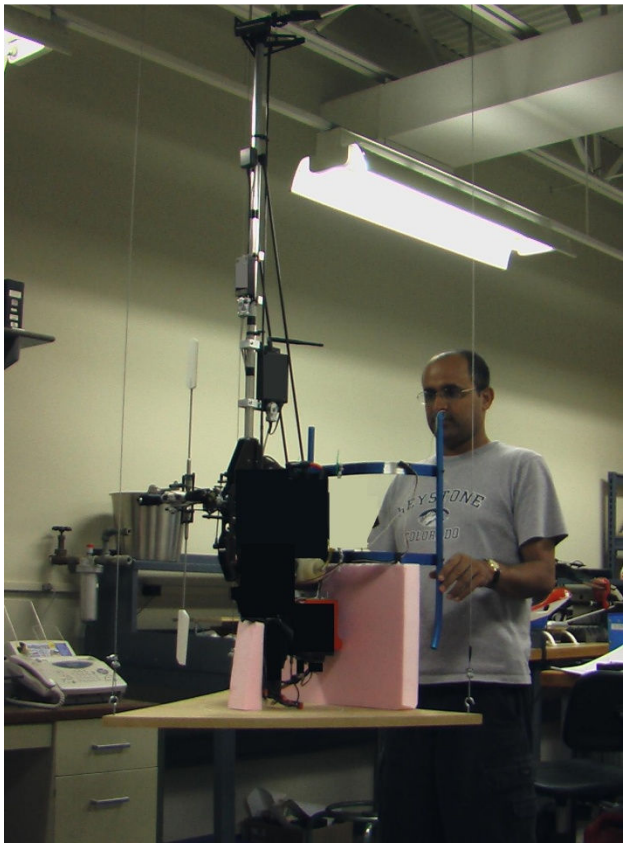

Figure 4-2: Pendulum Test Measuring Roll Moment of Inertia of a Helicopter UAV

Using the apparatus shown in Figure 4-3, the moment of inertia *J* is given by (Wagner & Cooney, 1979):

$$J = \frac{R^2 W}{4\pi^2 f_n^2 L}$$

where R is the radius from the center of the platform to the string, W is the weight of the test object and platform combined, f_n is the frequency in Hz, and L is the length of each string.

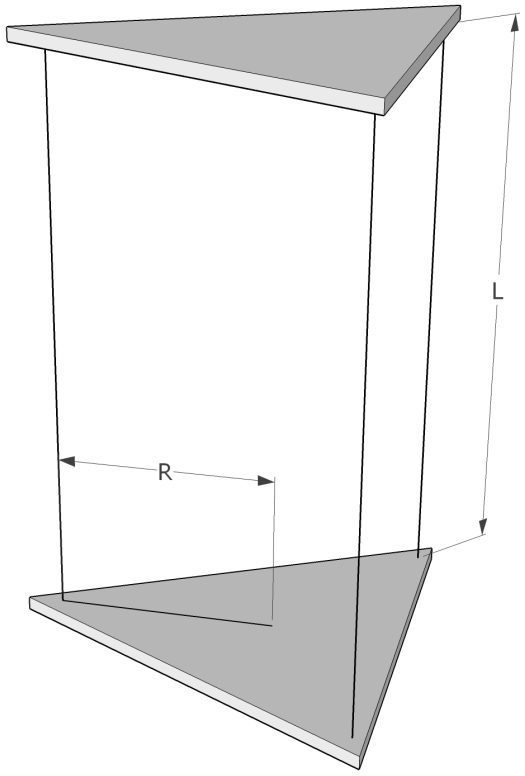

Figure 4-3: Three-String Torsional Pendulum

Table 4-2 gives the mass and location of the components of the modified model sailplane used in low altitude flight testing. Locations are given relative to a reference point, located 100 mm ahead of the nose and 500 mm below the center of the spinner. These component mass and location data are useful in software applications such as Advanced Aircraft Analysis (DARcorporation, 2006).

Table 4-2: Mass and Location of Components of the Low Altitude Test Aircraft

Component	Mass (g)	Distance from Reference Point (mm)		
		X	Y	Z
Modem	95	531	0	540
Battery (4000 mAh)	265	319	0	487
Computer / Sensors	125	478	0	496
Spinner and Props	35	119	0	496
Wing/Fuselage Fasteners	60	531	0	540
Airfoils	410	-	-	-
Wing Joiners	5	-	-	-
Aileron Servo	20	540	845	593
Aileron Servo	20	540	-845	593
Elevator Servo	22	593	27	473
Rudder Servo	22	593	-27	473
Fairings	9	327	0	549
Speed Controller / Wiring	40	310	0	496
Motor	181	150	0	496
Receiver	15	354	0	504
Battery (2100 mAh)	140	310	0	540

4.2 Parameter Estimation

In order to develop a useful and meaningful mathematical model and computer simulation of an aircraft, key parameters that describe the forces and moments acting on the aircraft must be measured or estimated with reasonable accuracy. Tools such as the U.S. Air Force's Stability and Control Digital DATCOM (Hoak & Fink, 1979) and DARcorporation's Advanced Aircraft Analysis software (DARcorporation, 2006) will be useful for estimating stability and control derivatives and coefficients based on the aircraft's geometry, c.g. location, and flight condition. However, the validity of those estimations remains a question. Both DATCOM and AAA rely on empirical data collected primarily from manned aircraft that are much larger, heavier, and operate at

lower altitudes compared with the UAV in this project. Low Reynolds numbers can have a significant impact on flight characteristics, as observed by Sim (Sim, 1984), Greer et al. (Brion, Aki, & Shkarayev, 2006), Selig (Selig & Guglielmo, 1997), and many other researchers. Also, both DATCOM and AAA require the user to simplify and approximate the actual aircraft parameters as inputs to the software. These simplification assumptions and approximations result in errors in the output.

Designers of small and micro UAV control systems anticipate errors in the estimated parameters, as shown in the following three examples. As the first example, Jodeh, Blue, and Waldron (Jodeh, Blue, & Waldron, 2006) relied on open-loop flight testing to verify and refine the output of DATCOM for their Rascal 110 UAV, shown in Figure 4-4.

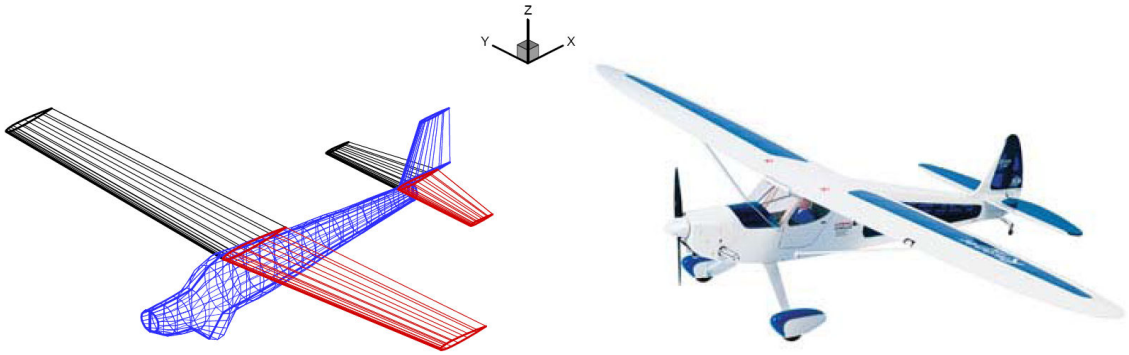

Figure 4-4: USAF Small UAV Research Platform, Rascall 110

(Jodeh, Blue, & Waldron, 2006)

Their research indicated that the "simulations tended to have less damped oscillations as compared to the flight test results" (Jodeh, Blue, & Waldron, 2006). An example of their flight test results compared to their simulation is shown in Figure 4-5. It is also noted

that the estimated period of oscillation differed from the flight test data.

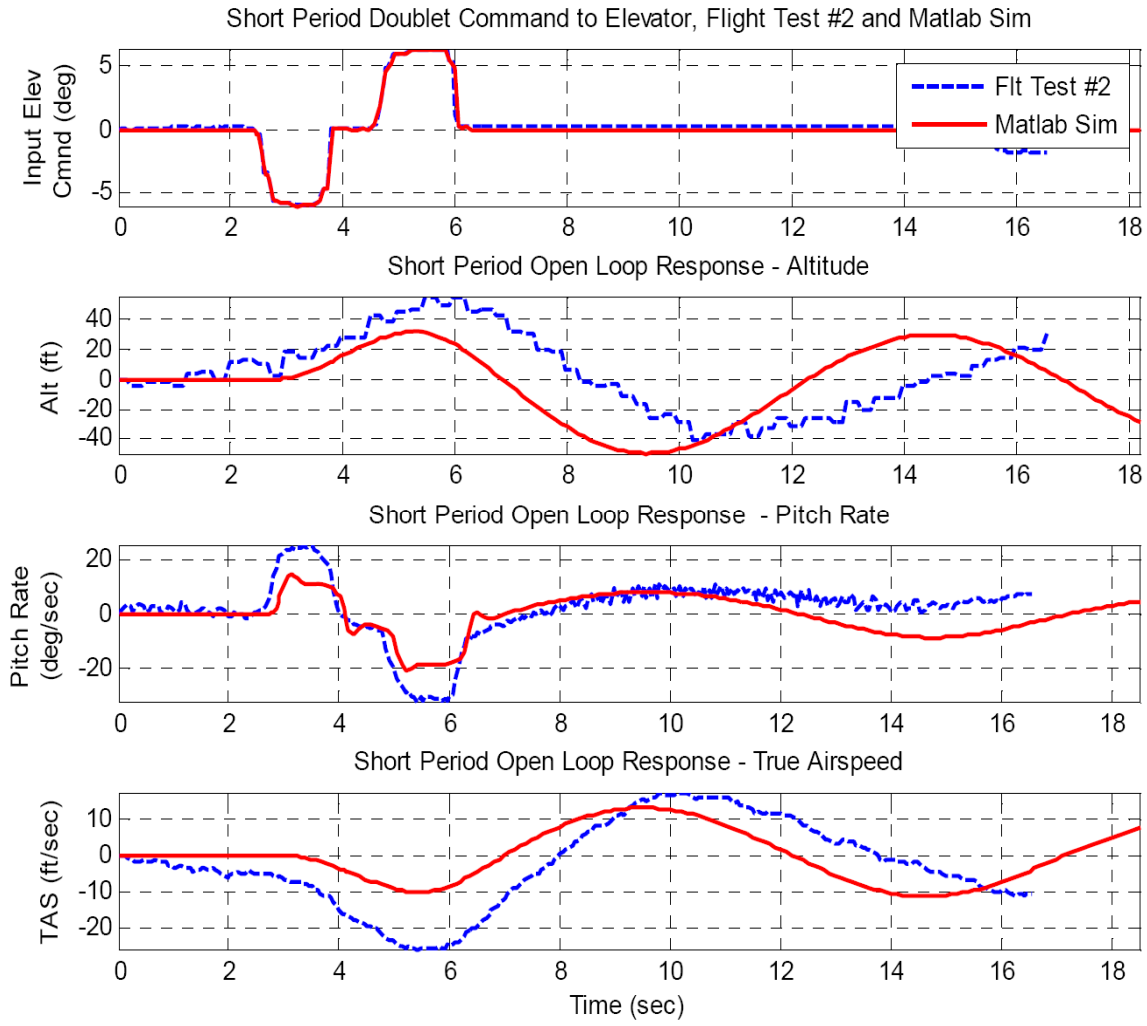

Figure 4-5: Flight Test Data vs. Simulation of the Rascal 110 UAV

(Jodeh, Blue, & Waldron, 2006)

As a second example, Krashanitsa et al. used AAA software to determine the aerodynamic derivative coefficients for the Zagi MAV from an input of airfoil and geometric data, as well as center of gravity location (Krashanitsa, Platanitis, Silin, & Shkarayev, 2006).

Table 4-3: Zagi MAV Specifications

(Krashanitsa, Platanitis, Silin, & Shkarayev, 2006)

Parameter	Zagi MAV
Wingspan (cm)	59
Length (cm)	31
Height (cm)	6
Wing area (cm^2)	885
Elevon area (cm^2)	300
Winglet area (cm^2)	80
Elevator area (cm^2)	-
Fin area (cm^2)	-
Rudder area (cm^2)	-
CG location from apex (cm)	12.7

An image of the Zagi MAV is shown in Figure 4-6. This aircraft flies at very low Reynolds numbers in the neighborhood of 1.2×10^5 when operating at a velocity of approximately 9 m/s (30 ft/s) (Platanitis & Shkarayev, 2005).

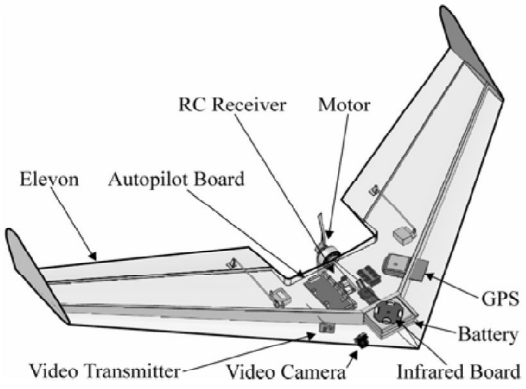

Figure 4-6: Components of the Zagi MAV

(Krashanitsa, Platanitis, Silin, & Shkarayev, 2006)

This paper (Krashanitsa, Platanitis, Silin, & Shkarayev, 2006), also contains a valuable

discussion of several other MAV controller development projects by a variety of teams that utilize low cost avionics systems. Anticipating discrepancies between the AAA estimates and the actual performance of their MAV, the research team also utilized vortex-lattice computational methods and Tornado software (Melin, 2001), (Krashanitsa, Platanitis, Silin, & Shkarayev, 2006).

In similar research, Platanitis and Shkarayev predicted longitudinal stability and control derivatives for a Zagi MAV using AAA software and compared those results to wind tunnel tests (Platanitis & Shkarayev, 2005). The results of the Platanitis and Shkarayev experiments are shown in Table 4-4.

Table 4-4: AAA Predictions vs. Wind Tunnel Tests of a MAV

(Platanitis & Shkarayev, 2005)

Parameter	Experimental Value	Predicted Value	% Error |Exp. – Pred.|/Pred.
$C_{D\_\min}$	0.02812	0.01631	72
$C_{D\alpha}$	0.07245	0.2108	66
$C_{D\delta e}$	0.009368	0.3045	97
C_{Lwo}	0.1696	0.09167	85
$C_{L\alpha}$	3.5722	3.5016	2.02
$C_{L\delta e}$	0.6238	0.2724	129

They conclude: “The large errors between the measured and predicted values of the aerodynamic coefficients clearly show that refinements in the experimental procedure are needed” (Platanitis & Shkarayev, 2005). Some possible sources of error in this experiment include wind tunnel experimental methods, geometry measurements, inertia

estimations, and assumptions made in the AAA software design.

As the third example, the APEX program at NASA's Dryden Flight Research Center designed a UAV to drop from a balloon at high altitude for the test and evaluation of low Reynolds number airfoils, propellers, and other technologies (Murray et al., 1992), (Greer, Hamory, Krake, & Drela, 1999), (Past Projects - APEX, 2006), (Lee, Bjarke, Greer, Tatineni, Zhong, & Jacobson, March 25-26, 1998), (Colozza, APEX 3D Propeller Test Preliminary Design, Sept. 2002). The APEX project aimed to lift a modified sailplane to high altitude using a balloon; the flight profile is depicted in Figure 4-7.

The APEX team developed an aerodynamic model using "a combination of computational techniques, wind-tunnel test results…, flight test results, and handbook methods" (Murray et al., 1992). The NASA team used software and a panel model, shown in Figure 4-8, of the APEX aircraft to estimate its longitudinal parameters.

The longitudinal model is most significant in this case due to the critical pull-out maneuver that immediately follows separation of the aircraft from the lifting balloon. Fixed wing airplanes generally experience two primary oscillations. These are well-known as the phugoid and the short period modes. The phugoid mode affects speed and pitch angle while angle-of-attack is constant. The short period mode affects mostly angle-of-attack and pitch angle while speed is constant.

The phugoid mode trades speed with altitude in a cycle between kinetic and potential energy. The phugoid can be estimated from speed alone. Both the high altitude Mars

demonstrator and the low-altitude avionics test aircraft have high L/D, which indicates that the phugoid will be lightly damped (Roskam, 1991). The short period undamped natural frequency of an airplane depends primarily on the distance from the AC to the c.g. (Roskam, 1991).

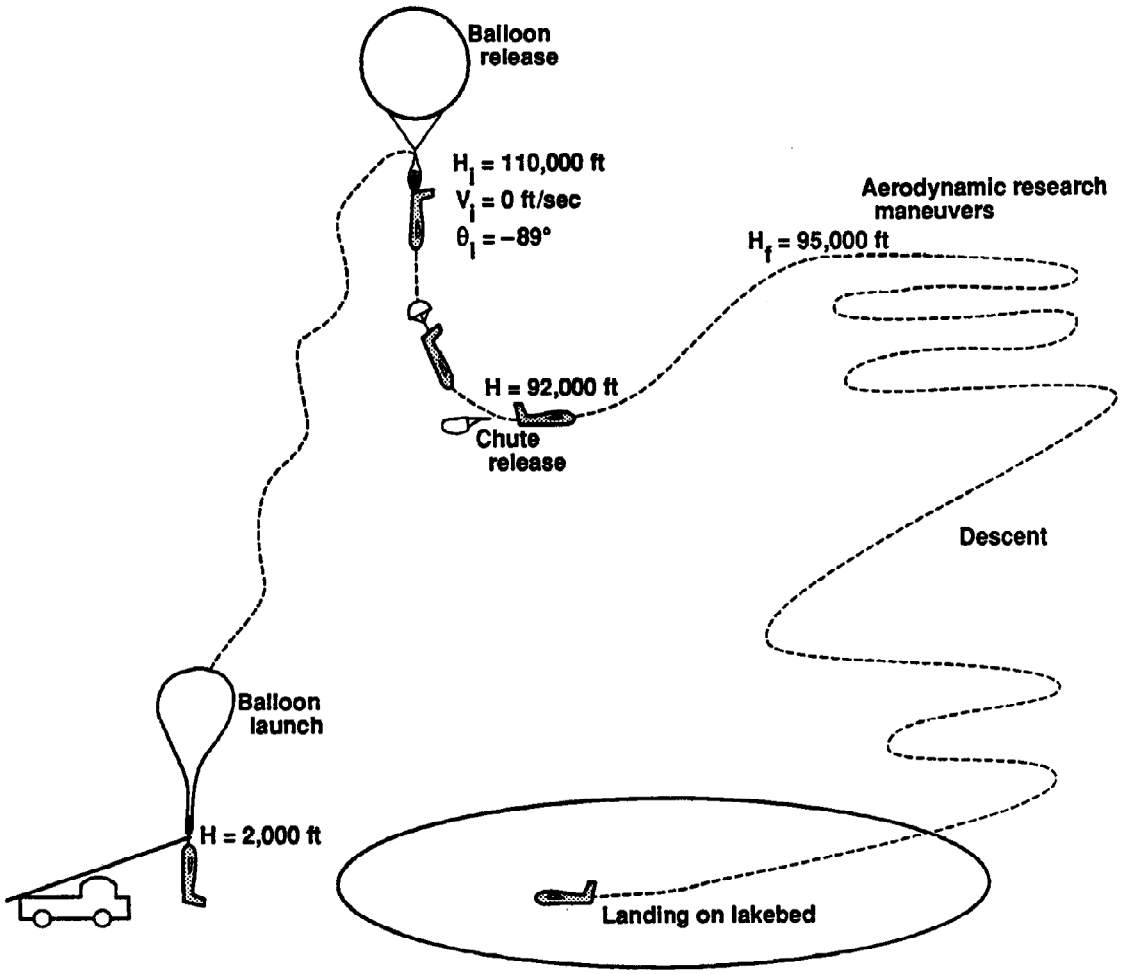

Figure 4-7: NASA's APEX Flight Test Concept

(Murray et al., 1992)

If simulations predict that the high altitude UAV will accelerate to transonic speeds before completing the pull-out, then an alternative method of dropping from the balloon should be considered. One possibility that looks promising is releasing the aircraft at a nose-down pitch angle of about -20 to -40 degrees in order to start the flight in a controlled deep stall. The UAV could subsequently transition to normal flight without accelerating as fast as in a dive like that of the APEX aircraft.

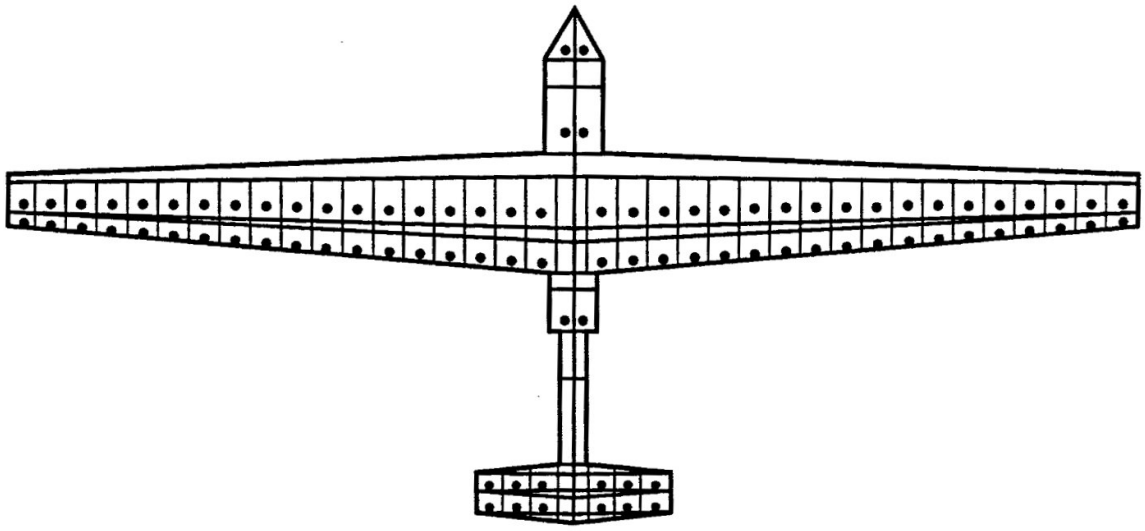

Figure 4-8: LinAir Panel Model of NASA APEX Aircraft

(Murray et al., 1992)

In the 1980s, a team at the NASA Dryden Flight Research Center conducted a series of flight tests with a modified sailplane to investigate its flight characteristics and controllability in a deep stall, as shown in Figure 4-9 and Figure 4-10.

The NASA test airplane was a modified SGS 1-36 sailplane. The original T-tail was modified so that the entire horizontal tail (stabilator) could move from 0 deg to a 70 deg

trailing-edge-up position, controlled by the pilot with a lever installed in the cockpit (Sim, 1984). This large deflection of the stabilator, visible in Figure 4-10, allowed the pilot to transition from normal flight into a controlled deep stall and recover safely (Sim, 1984). The pilot's lever for the stabilator had several stops so that the stabilator incidence angle remained fixed for each descent (Sim, 1984). The NASA team found that the aircraft would stabilize at angles of attack between 30 and 72 deg, depending on the elevator and stabilator positions, with a near-zero pitch angle (Sim, 1984). The descent rate usually stabilized at about 20 m/s (4,000 ft/min) (Sim, 1984).

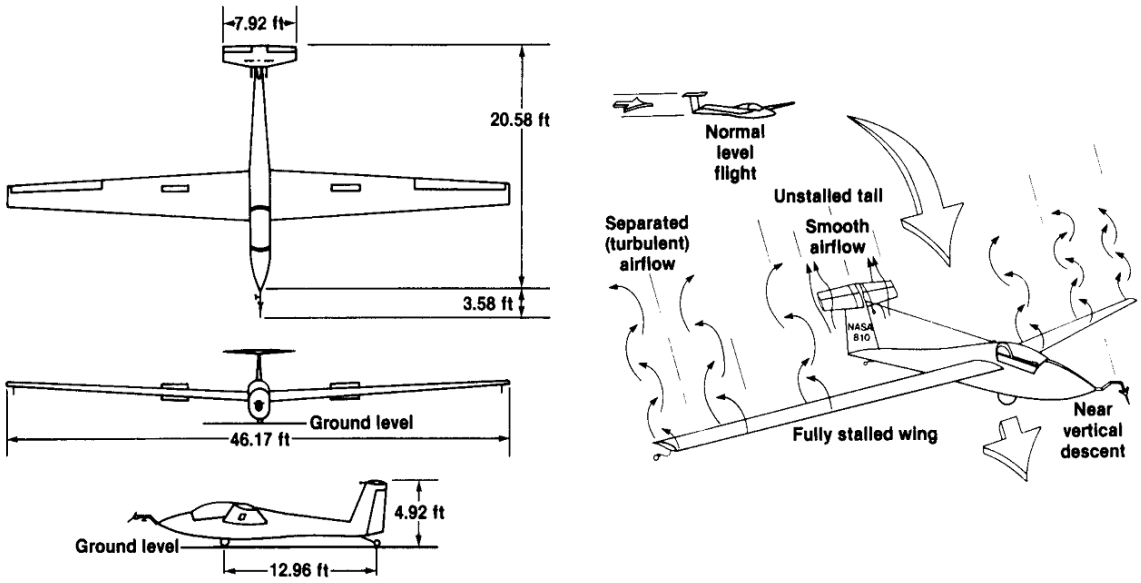

Figure 4-9: NASA Controlled Deep Stall Flight Test Concept

Sim gives a concise overview of the deep stall flight tests, but Mahdavi and Sandlin's report contains extensive detailed data. The plot shown in Figure 4-11 has been redrawn because the archived report was in poor condition.

Figure 4-10: NASA Controlled Deep Stall Flight Testing

(NASA Photo: ECN-26847, 1983)

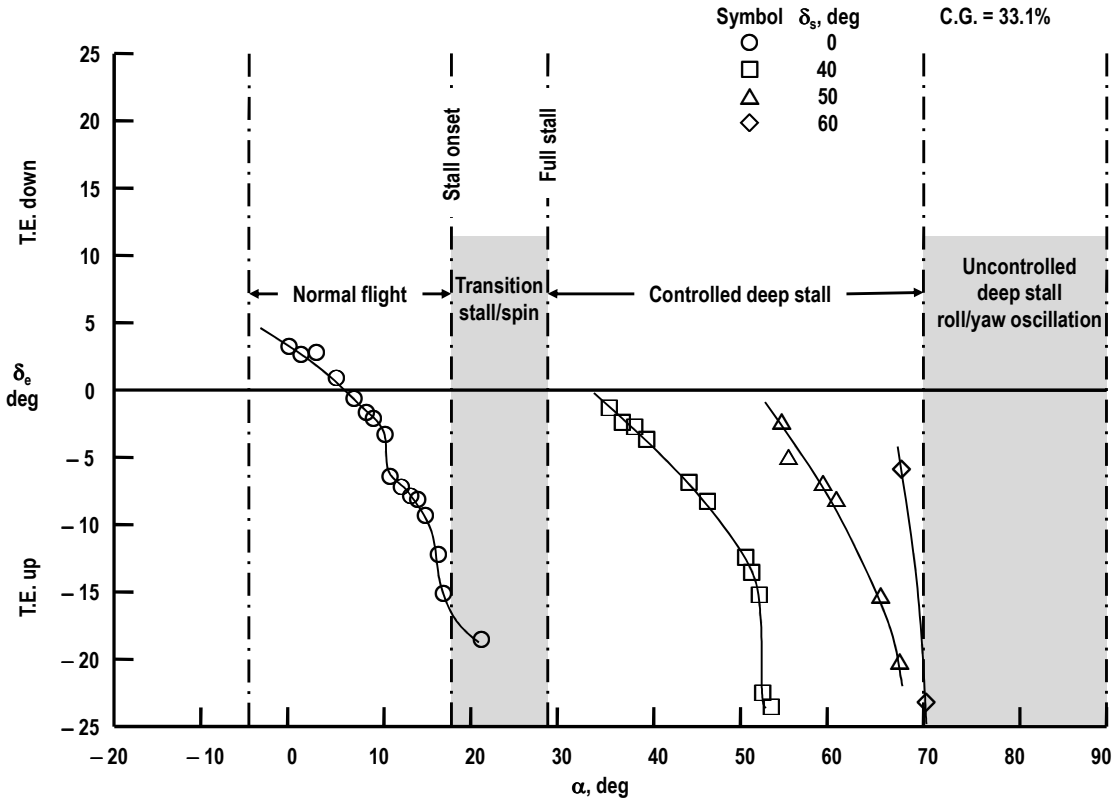

Figure 4-11: Sailplane Deep Stall Flight Determined Trim Data

(Mahdavi & Sandlin, 1984, p. 62)

For small UAVs, the large negative stabilator incidence angles can be controlled with a combination of proportional and retract servos. The proportional servo will control the pitch of the aircraft during normal flight, but it will be mounted on rails in a mechanical mixer. The proportional servo will slide on the rails from the standard position at one end to the deep-stall position at the other end. This sliding action will be controlled by the retract servo, as illustrated in Figure 4-12. Therefore, the retract servo will be used to transition from normal flight to deep stall and back again in a fashion similar to the pilot's lever in NASA's modified SGS 1-36. The action of the proportional servo is analogous to the elevator control on the SGS 1-36. This concept for mechanically mixing the actions of two servos eliminates the complexity of hinged elevators mounted on variable-incidence stabilators on a small UAV.

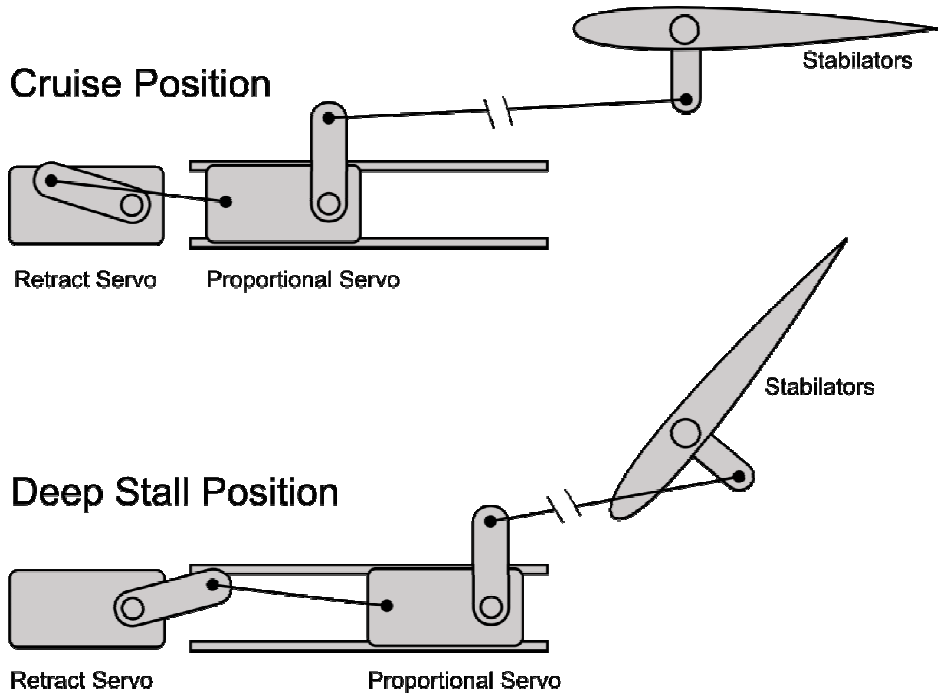

Figure 4-12: Servo Arrangement for Controlled Deep Stall Flight

5 Simulation

Early conceptual simulations of the high altitude balloon drop and pull out were conducted using X-Plane flight simulation software. The X-Plane software package includes a CAD utility called Plane-Maker which allows the user to model the geometry of an aircraft. Additionally, the user specifies the c.g. location, control surface parameters, propulsion parameters, and other data relevant to the simulation.

A model of the KU high altitude UAV was created for piloted simulation study, which is shown in Figure 5-1. The high incidence angle of the all-moving canards during the pull-up is visible in the screenshot.

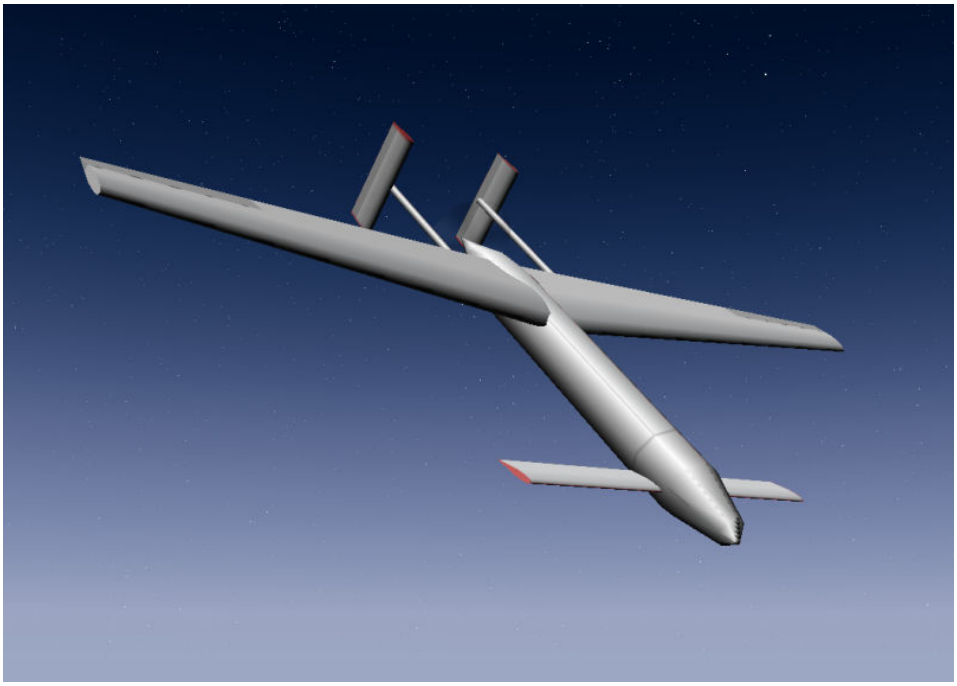

Figure 5-1: High Altitude UAV Simulation Model in X-Plane

The X-Plane software evaluates the dynamics of the aircraft using blade element theory

(Laminar Research, 2007). According to the X-Plane Web site, the software loops through the following four steps at least 15 times per second:

1. Each of the airfoils is broken-down into at most 10 elements per side.
2. The aircraft's linear and angular velocities and the relative position of each element are used to find the velocity vector of each element, considering the effects of downwash, propwash, and induced angle of attack from lift-augmentation devices.
3. 2D airfoil data and appropriate finite-wing reductions are used to determine the lift, drag, and moment coefficients for each of the airfoils.
4. Dynamic pressure is calculated for each element, and using the coefficients and areas found in previous steps, the forces are calculated and summed for the entire aircraft. Dividing by the mass or an applicable moment of inertia, the linear and angular accelerations are found.

The APEX simulation used a panel method (see page 42), which is similar to the blade element method implemented by X-Plane. The X-Plane software allows the user to initialize the simulation at any altitude, location, and forward speed. However, the attitude and vertical speed are always initially zero. Therefore, the simulations used to evaluate the high altitude UAV's drop from a balloon begin with the aircraft at 34,600 m (114,000 ft) with zero velocity and the fuselage horizontal (zero pitch angle). In the first few moments of the simulation, the aircraft begins falling and pitches downward to nearly -90 deg. This initial condition is different from the flight test design. During the

high altitude flight test, the aircraft will be suspended by the tail, so the initial pitch will be approximately -89 deg.

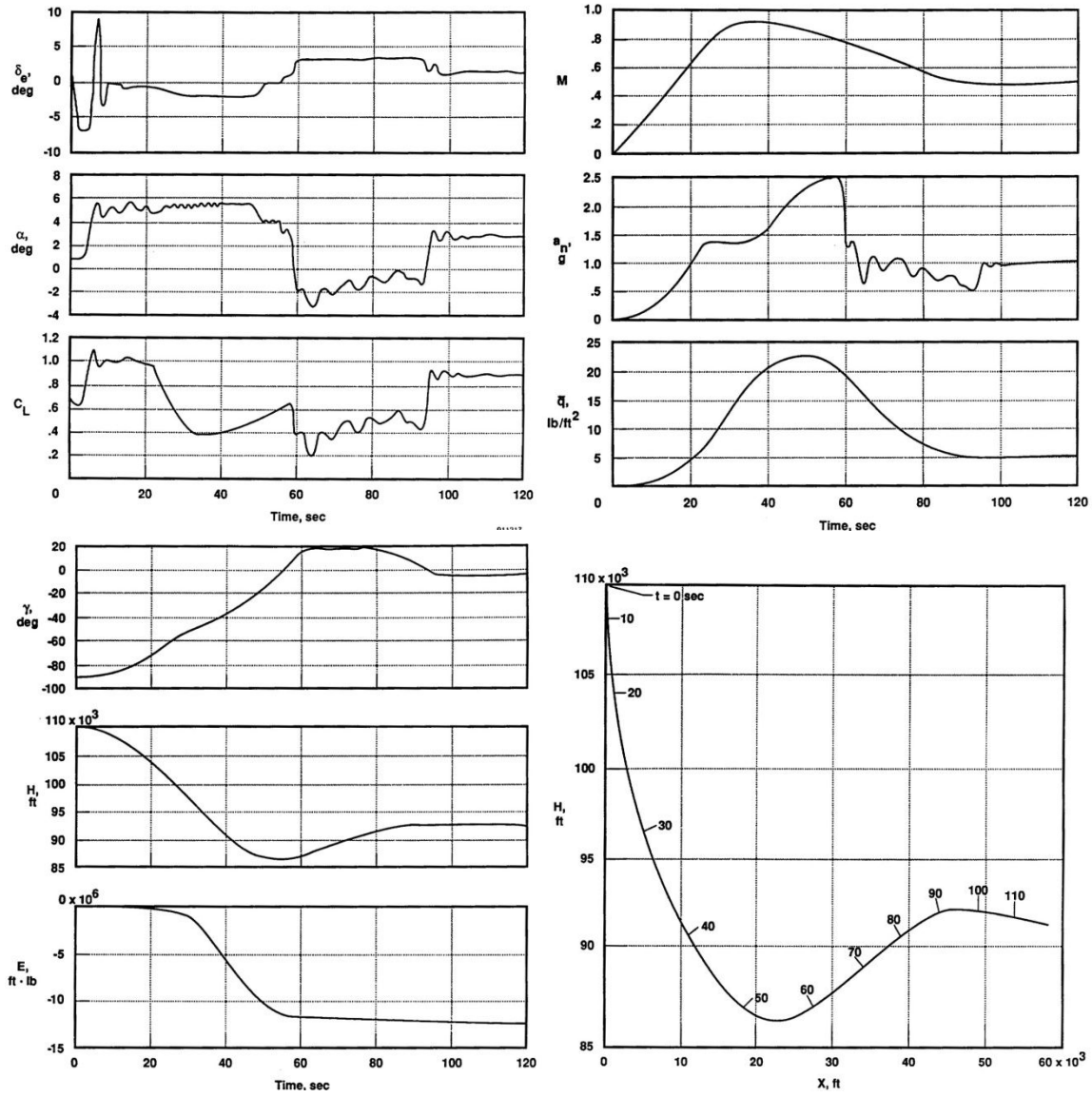

Figure 5-2: Plots from an APEX Balloon-Drop Simulation

(Murray et al., 1992)

This simulation setup was repeated multiple times with a human pilot attempting to

transition the aircraft to level flight. This method of letting a human pilot learn a reasonable control technique through simulation was previously used by the APEX team at NASA to begin the design of the aircraft's intended trajectory (Murray et al., 1992). The plots in Figure 5-2 show the results of the APEX simulation by Murray et al. in 1992.

After several repetitions of the balloon-drop simulation, the human pilot learned to successfully transition from the dive to level flight. An example of a successful trajectory is shown in Figure 5-3.

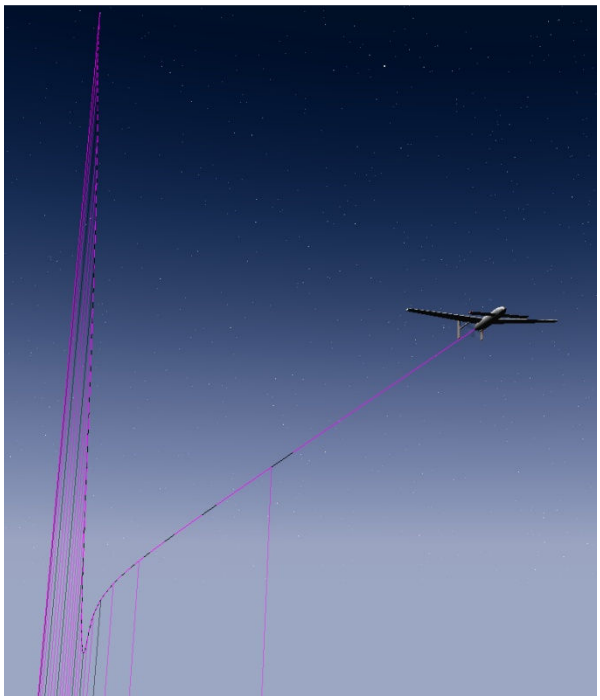

Figure 5-3: Simulated Trajectory of Transition to Level Flight

The vertical lines in Figure 5-3 and Figure 5-4 indicate 1.00 sec intervals of time. Remarkably, the built-in autopilot feature of X-Plane was capable of executing a very similar maneuver without any special autopilot mode or software configuration. No

documentation about the methods or theory behind the X-Plane autopilot could be found.

Figure 5-4 shows one of the successful trajectories from a view orthogonal to the vertical plane of the pull-out maneuver. At the lowest point of the flight path, the pilot continues to pitch up into a climb in order to reduce the airspeed to the trim cruise speed.

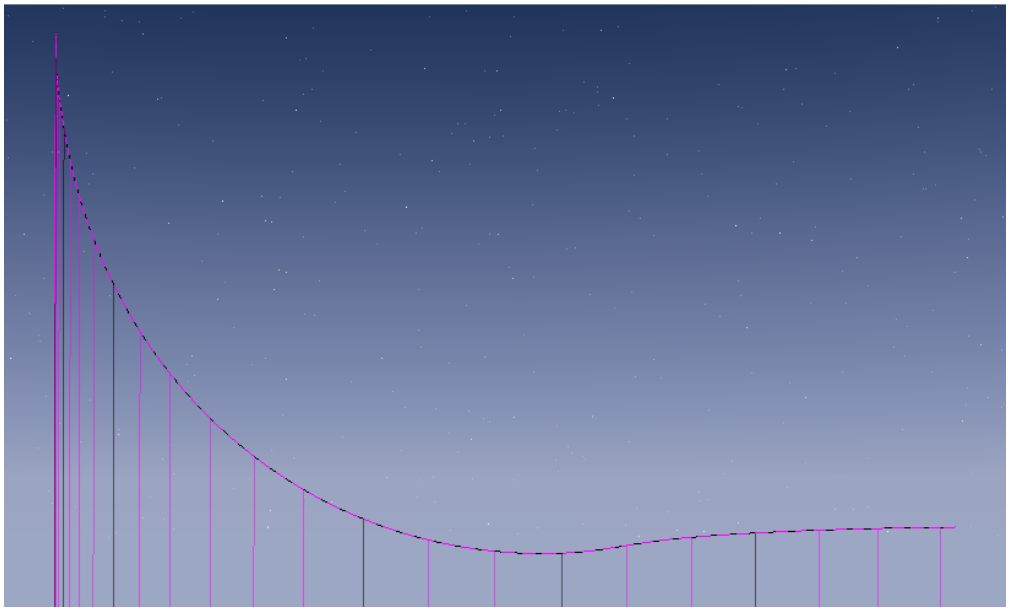

Figure 5-4: Simulated Trajectory, Viewed from the Side

The data output from X-Plane was imported into MATLAB and used to generate the plot in Figure 5-5. The location of the origin of the *x* and *y* axis is unknown, but is irrelevant to the simulation.

The simulations indicated that a successful pull-up maneuver would end in level flight approximately 1,100 m (3,600 ft) below the point of release. The load factor during the pull-out peaked between 2 and 3 G in most of the simulations.

NASA simulations of the larger APEX aircraft predicted a loss of altitude of about 5,500 m (18,000 ft) as shown in Figure 5-2 (Murray et al., 1992). However, the maximum load factors of both the KU high altitude UAV and the NASA APEX aircraft in each of these simulations was about 2.5 G.

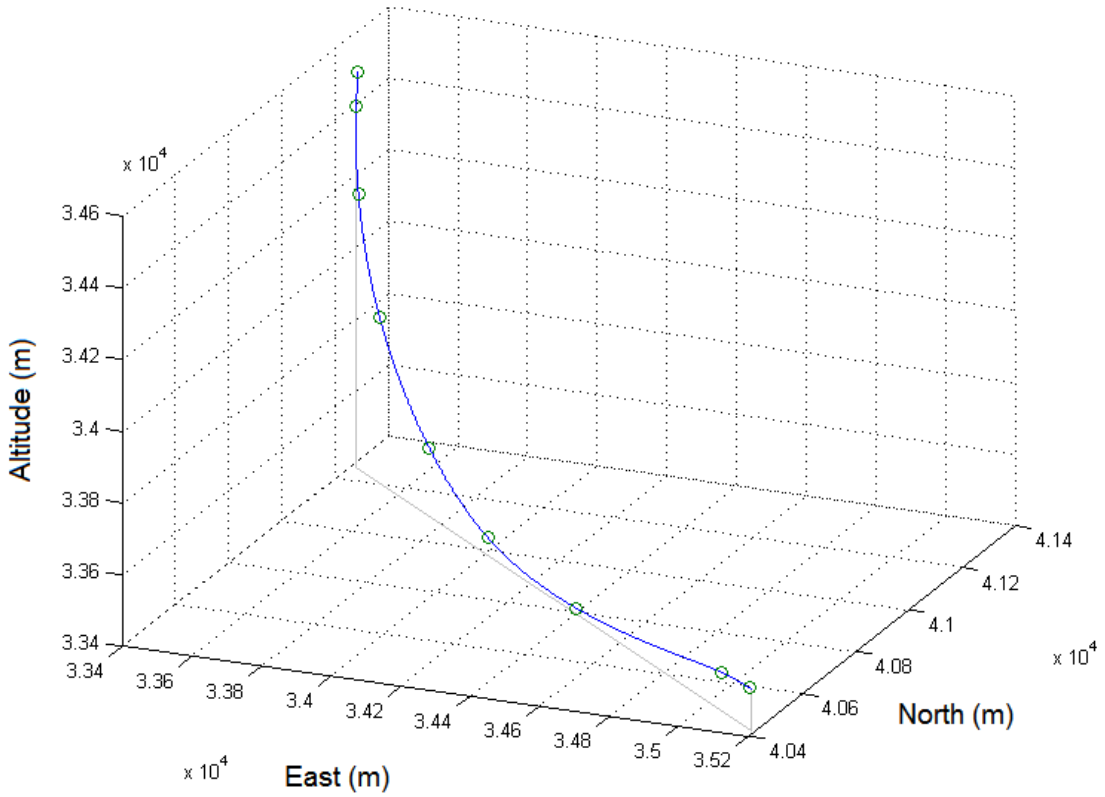

Figure 5-5: X-Plane Simulation Output in MATLAB

Note that the APEX aircraft reaches airspeeds as high as 0.9 Mach. The KU high altitude UAV did not exceed 0.3 Mach in these simulations. The APEX aircraft was not simulated with X-Plane for comparison because the X-Plane blade element analysis does not model transonic effects (Laminar Research, 2007).

6 Controller Design

The detailed design of the high altitude UAV will depend on the finalized design of the aircraft. The preliminary controller design will be possible when the geometry and structure of the aircraft are finalized. The final controller design will likely depend on the completion of wind tunnel testing to measure some parameters that are difficult to predict analytically. For example, the downwash angle at the horizontal tail can be tricky to predict without testing (Anderson, Introduction to Flight, 5th ed., 2005).

After separation from the balloon, the aircraft will accelerate downward and dynamic pressure will increase until adequate control authority is obtained. The aircraft will begin a steady pull-out. At the end of this maneuver, the aircraft will level off at cruise speed.

The maximum loads on the aircraft's structure are expected during the pull-out maneuver. Therefore, one of the key requirements of the controller is that the pull-out should not exceed the load factor estimated by the design team. However, if the pull-out is too slow, the aircraft might accelerate to a transonic airspeed, such as NASA simulations predicted for the APEX airplane (see Figure 5-2). This could lead to catastrophic failure of the aircraft's structure.

The high altitude flight test will take about 4.5 hours from balloon launch to recovery, and the avionics must be in operation from prior to the launch through touching down. Therefore, the controller must be designed to minimize energy consumption by the actuators. The flight management system should also monitor the battery voltage. If the

rate of data streamed to the ground station is reduced, the radio modem will consume less power. The flight management system should reduce the data rate if the battery voltage is low to increase the endurance of the avionics.

Since the high altitude flight conditions cannot be replicated in human-piloted testing, the controller must be designed using analytical tools only. Therefore, the controller must be designed with uncertain parameters. Also, there is very little information about high altitude weather conditions. On the day of the launch, there will be significant uncertainty about the temperature, wind speed, and other conditions. To mitigate risk during the flight test, the robustness of the controller is essential.

Based on previous experience with FAA authorities, even with a special waiver, the maximum permissible weight for the high altitude balloon payload is 5.4 kg (12 lbs) (see p. 27 for details). This weight limit leads to a small UAV design. The nature of the mission to Mars also places extreme constraints on mass and volume. Avionics hardware must be light, and power consumption must be minimal. Therefore, a small form-factor embedded computer is chosen to be the heart of the flight test system. Specifics about the hardware are described in Section 7.2. The controller must be implemented for this embedded target. The software must be sufficiently simple to execute with limited RAM and a 400 MHz Xscale processor. The executable binary files must be sufficiently compact to occupy limited flash memory onboard the Stargate SBC.

The analog sensors are sampled at 50 Hz, while the GPS updates at 4 Hz. The controller must be designed with the effects of discrete-time sampling in mind.

It is suggest that the pull-out maneuver should be controlled by feeding back the flight path angle γ to the canards or stabilators. After cutting the aircraft free from the balloon, γ will be about -89 deg. The commanded γ should ramp up past zero to +10 or +20 deg to reduce the speed of the aircraft. Finally, γ should ramp back down to zero degrees. At this point, control should transition to a typical altitude-hold method. When the trimmed cruise condition is stabilized, the controller should begin sending open-loop doublet commands one at a time to each of the three flight control axes.

An alternative method for controlling the transition to level flight would be to feedback the vertical acceleration $\dot{w}$ to the canard or stabilator. The APEX controller was designed to use the load factor (vertical acceleration) as the primary feedback during the transition to level flight (Lee, Bjarke, Greer, Tatineni, Zhong, & Jacobson, March 25-26, 1998). The APEX team learned that measuring angle of attack and airspeed is challenging in low density air at high altitude. Also, since the aircraft used rockets aligned on the z-axis through the c.g., feeding back $\dot{w}$ to the elevators automatically took into account the contribution of the rocket thrust to the vertical acceleration. The vertical acceleration will be measured directly with an accelerometer, while air data states such as angle of attack and airspeed, must be estimated indirectly by integrating and filtering other measured states.

7 Systems Integration

The high altitude UAV flight test system will depend on the integration of several subsystems and multiple heterogeneous components. The overall goal of this system is to acquire flight test data and bring it back to the ground for later analysis. The flow of this information is illustrated in Figure 7-1. Each of the components is discussed in detail in Section 7.1. The software is just as essential as the hardware components. Implementation of the autopilot and data acquisition software is discussed in Section 7.2.

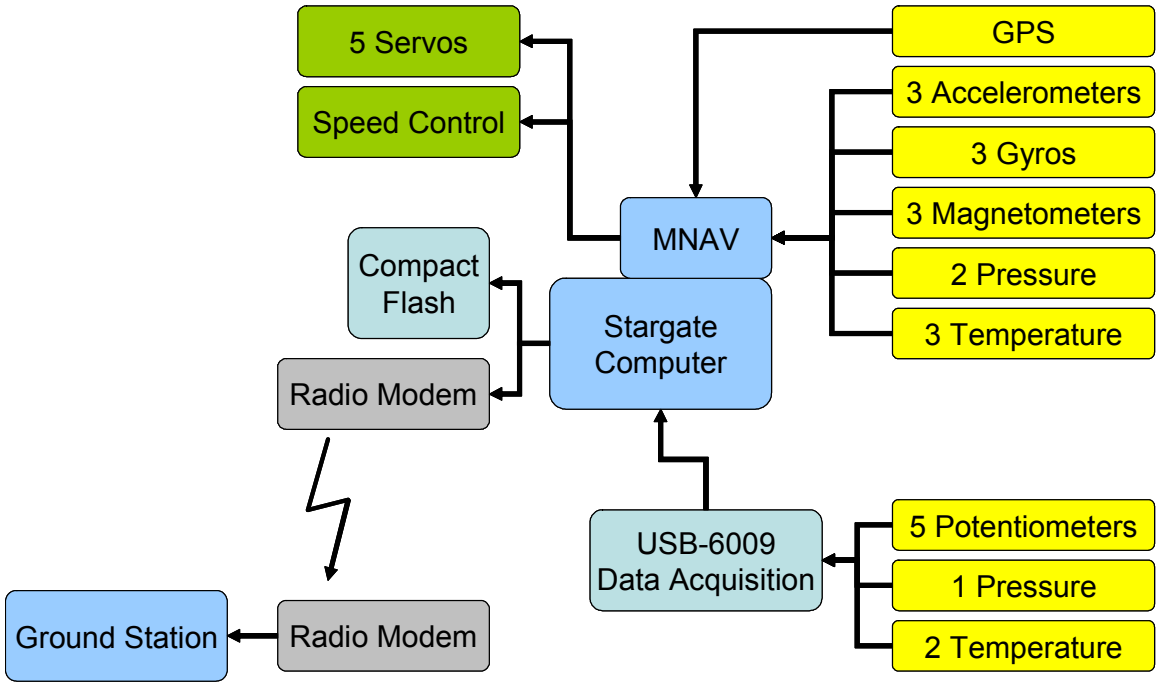

Figure 7-1: Components of the Flight Test System

7.1 Systems Design

The goal of the systems design is to satisfy the flight test requirements using low cost, light weight, and energy efficient components. The design is modular in the sense that

most of the components could be replaced with alternative solutions with minimal reconfiguration of the other components. For example, the 900 MHz radio modem could be replaced with a modem operating at a different frequency or with a different modulation scheme. If additional range is required, radio modems in the 144 MHz band can cover more distance but offer less data throughput and require FCC licensed operators. The modularity of the systems design provides flexibility in anticipation of revised mission requirements and possible re-use on future projects with new goals.

The disadvantage of this system is that it lacks redundancy. There are numerous single point failures that could interrupt the flight test. As a contingency, the recovery parachute is designed to deploy by two separate triggers, independent of the avionics. If the flight test electronics fail during the test, the parachute will either be triggered by a timer or an independent altimeter switch (Brown et al., 2006). This strategy helps maintain safety, but does not guarantee recovery of the UAV. If the telemetry stream is interrupted, the flight test team's chase vehicles will lose track of the UAV and will be unable to locate the landing site. As stated before, the aircraft should be clearly marked so that anyone who discovers the UAV will be able to contact the team.

The following sections describe each of the subsystem designs. Several of these systems have been tested at high altitude on previous balloon flights. Information about these field tests are presented in Section 8.

7.1.1 Power System

The KU Mars airplane concept uses electric propulsion. An electric motor will drive a propeller using battery power (Brown et al., 2006). The avionics and servos will rely on a separate battery (Brown et al., 2006). The concept is that the entire propulsion battery capacity will be expended performing doublets and frequency sweeps at high altitude, but the avionics and servos will be required to function well after those maneuvers have been completed as the UAV descends and lands.

Lithium-polymer batteries were selected by the KU Mars airplane design team because they carry the most capacity with the smallest mass (Brown et al., 2006). However, the performance of lithium batteries is severely limited in cold temperatures. The KU team planned to use chemical hand warmers to heat the batteries, as recommended by the XBS team.

Colozza arrived at a similar conclusion to the KU Mars airplane design team: "Ideally [the batteries] would be insulated to maintain them at a temperature of 0 to 20 deg C. However, during operation the insulation may cause the batteries to overheat since they will be drained at a fairly high rate which will cause significant internal heating" (Colozza, APEX 3D Propeller Test Preliminary Design, Sept. 2002).

After the University of Kansas Mars airplane design project concluded in December 2006, Eagle Picher Inc. continued to give advice regarding the design of the batteries for the flight test system. Eagle Picher designs, manufactures, packages, and tests batteries for

aviation and space applications. Tests conducted by Jeremy Burnison, an engineer at Eagle Picher, determined that insulated batteries did indeed overheat during a 10 minute high-current discharge similar to the propulsion system requirements of the high altitude UAV. However, the overheating was not substantial enough to burst the batteries or cause a fire. At worst, the overheating negatively impacts the cycle life of the lithium battery. That is, a battery that overheats will not be able to recharge as many times as a battery that operates within the design specifications. This is an acceptable trade off for this project, since the batteries will not be required to cycle but a few times.

Testing revealed that the chemical hand warmers used by XBS were effective at keeping the avionics box temperature sufficiently high (see page 80). The avionics box tested had an internal volume of about 5,000 cm^3 (300 in^3). Based on experience with the high altitude testing of the avionics, two chemical hand warmers were sufficient to maintain required temperatures.

7.1.2 Communications System

The aircraft's mission requires that the flight data be streamed in near real time from high altitude to the ground station. Winds aloft will push the balloon downrange. Therefore, the radio modems are required to have a line-of-sight range of over 64 km (40 miles).

A suitable solution was found in the 900 MHz band. The MHX920 produced by Microhard Systems Inc. has a 97 km (60 mile) line-of-sight range (Microhard Systems Inc., 2007). The modem module and development board is shown in Figure 7-2.

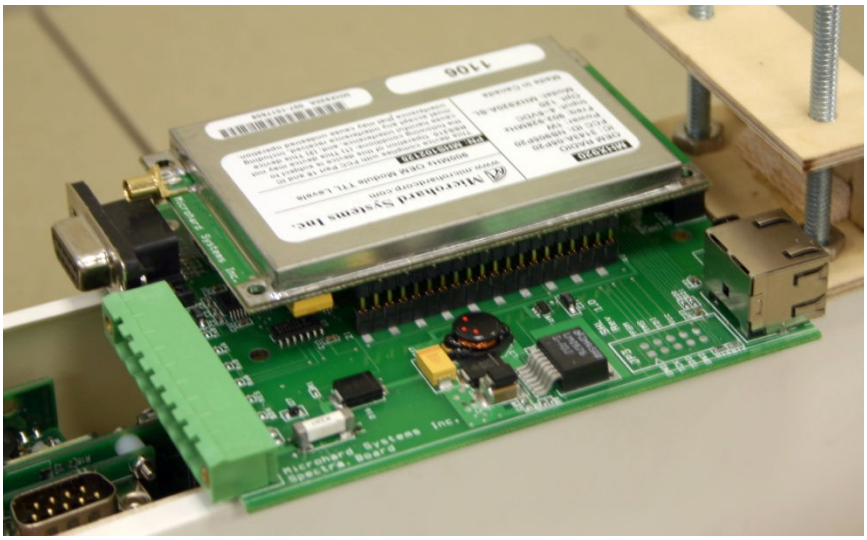

Figure 7-2: Radio Modem Module and Development Board

The radio modems utilized in this design can be reconfigured for several multi-node topologies. The best topology for this application is point-to-multipoint, where the aircraft's modem is the central host, and the ground station modems are clients. In this arrangement, the telemetry transmissions from the UAV will be received by all the ground stations within range.

The 900 MHz band is attractive because it is unlicensed and the hardware is relatively low cost. However, the FCC limits on transmit power prevent most 900 MHz radio modems from having the required range. Using frequency hopping spread spectrum techniques, the MHX920 has a sensitivity of -110 dBm. This means that the aircraft's communications antenna can be a simple dipole, as long as the ground station has a high-gain directional antenna properly pointed toward the aircraft. Testing of the modems during the HABS-16b flight demonstrated that even a simple monopole antenna on the chase vehicle's roof was sufficient for good reception.

The selected radio modem has a throughput as high as 230.4 kbps, but for this application the data rate will be reduced to 19.2 kbps in order to improve the reliability of the connection at long range. The design for the data stream allows for two 32-bit channels for latitude and longitude, and fourteen 16-bit channels for states at a sample rate of 50 Hz. This stream totals 14.4 kbps, which allows for some error-correction overhead on the signal. To conserve energy, the modem will transmit in intermittent pulses during the descent phase of the mission.

By enabling forward error correction (FEC), the individual packets of data can be checked for validity and sometimes even reconstructed if some of parts of the data were corrupted. FEC eliminates the need to retransmit corrupted packets. Therefore, the stream of data continues and the packets are delivered as soon as possible. Enabling FEC requires some overhead, so the total throughput of the modem is reduced. The MicroHard radio modems support multiple FEC methods. All of the modems in the network must be configured to use the same FEC method. For testing, the modems were configured to use a default FEC method; however, another method may be more appropriate for this application. Additional investigation is required.

The modems were tested on the bench to measure their power consumption. The modems were configured specifically as they would be operating during the high altitude flight test. The modems were configured to use maximum transmit power, regardless of signal strength, and the modems' forward error correction methods were enabled. The maximum power consumption was observed when the modem was transmitting during a

file transfer. The lab DC power supply provided 8.0 V and the modem drew 700 mA while sending a file (varying between 660 mA to 750 mA). Therefore, the modem was using 5.6 W, sometimes increasing to 6.0 W. Minimum power consumption was observed while the modem was idle, neither sending nor receiving data, and at idle was constantly drawing 220 mA at 8.0 V, or about 1.8 W.

The radio modem's power consumption is certainly related to the data rate demanded, but the specific relationship could not be identified without additional testing equipment. The aircraft's flight management software streams data constantly during the ascent and flight test. During the descent phase, data is sent intermittently in bursts in order to reduce the energy consumed by the modem while still providing location information to aid in recovering the aircraft after touchdown.

7.1.3 Sensors

In order for the autopilot to control the aircraft and transmit flight data to the ground station, the avionics system must be able to estimate the state of the aircraft. The design includes a low cost, lightweight sensor package that measures each of the key parameters.

In the current design, the sensors are contained in a device called MNAV, which is designed and manufactured by Crossbow Technology Inc. The MNAV sensor package includes accelerometers, angular rate sensors, magnetometers, static and dynamic pressure sensors, and a GPS sensor.

The MNAV is not rated for the cold temperatures expected during the high altitude flight

test. However, the thermal system described in Section 7.1.1 has been proven to maintain temperatures above 30 deg C (86 deg F) throughout the flight profile. See Figure 8-6 for the results from the high altitude balloon flight. Maintaining temperature is essential to battery performance as well as the functionality of the MNAV.

The rate gyros and accelerometers are based on MEMS technology. These components are low cost, but are easily saturated and have higher levels of noise when compared to larger, heavier, and more expensive instruments. The accelerometers become saturated at ±2 G, and the gyros have a range of ±150 deg/sec. These sensors are subject to drifting bias. Therefore, a GPS tie-down method is used to estimate the states.

In addition to the sensors, the MNAV also includes a 9-channel servo controller. The MNAV provides data output via an RS-232 serial link. The MNAV is designed to connect with Crossbow's Stargate single board computer discussed in the next section. A block diagram of the MNAV device is shown in Figure 7-3.

Measuring airspeed by a Pitot-static pressure system is infeasible at high altitude, due to the lack of small-scale, high-sensitivity differential pressure transducers. The static pressure at 110,000 ft is about 692 Pa (14.5 lbs/ft^2). The aircraft's speed will vary between 50 m/s (97 knots) and 100 m/s (195 knots), so the dynamic pressure will range from 13 Pa (0.27 lbs/ ft^2) to 52 Pa (1.09 lbs/ ft^2). The MNAV's built-in pressure sensors are not sensitive enough to accurately measure these pressures and will not be adequate for measuring altitude and airspeed in the upper atmosphere. Therefore, the flight test team will connect a separate pressure transducer to the data acquisition board to measure

altitude, and the airspeed will be estimated from the GPS information. Several PC board mountable pressure sensors exist that are useful for measuring altitude. One example is the Omega PX40 (Omega Engineering Inc., 2006).

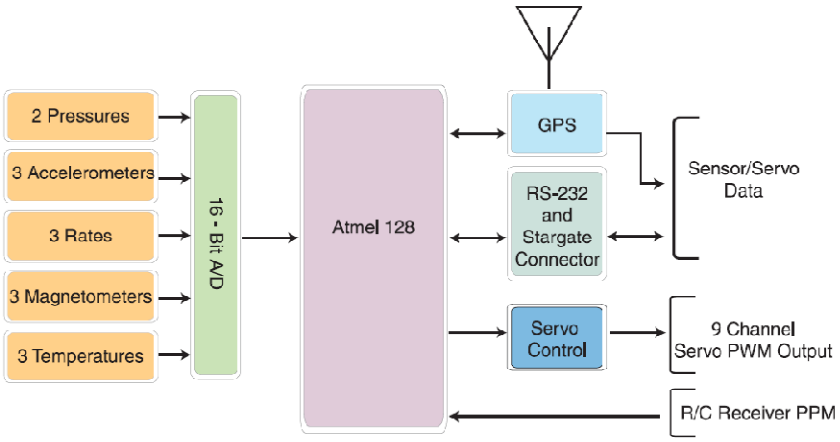

Figure 7-3: MNAV Block Diagram

(Crossbow Technology, Inc., 2006)

For airspeed to be estimated from GPS, the wind direction and magnitude must be known. Just prior to release from the balloon, the balloon and aircraft will be drifting along with the winds. Therefore, GPS may be used to estimate the wind velocity. The flight test team will assume that the wind will remain nearly constant for the subsequent flight test. Therefore, the ground speed measured by GPS prior to separation from the balloon will be used to estimate wind velocity. Wind is assumed to be constant throughout the flight test, which is completed in less than 10 minutes.

In addition to the vehicle states measured by the MNAV, the flight test requirements mandate that the control surface deflections must also be recorded. Therefore, an

additional analog to digital conversion device will be added to the avionics. A suitable solution is the National Instruments USB-6009. This device digitizes 8 channels at a 14 bit resolution at sample rates up to 48 kHz. The data will be sent to the flight computer over a USB connection.

If the high altitude UAV uses a similar planform to the University of Kansas design from 2006, five potentiometers are required to measure the deflections of the control surfaces (Brown et al., 2006). These sensors will be located adjacent to each of the control servos. The wiring to connect the sensors to the data acquisition board is shown in Figure 7-4. Data gathered from these sensors will allow the flight test team to incorporate the dynamics of the servos into the overall aircraft model.

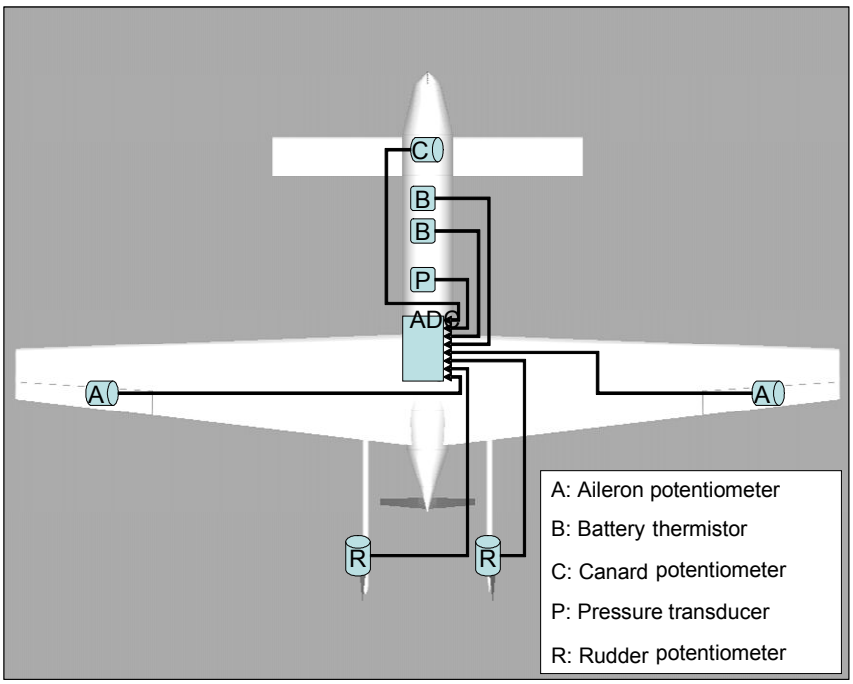

Figure 7-4: Sensor Locations on the KU Mars Airplane Design

7.1.4 Actuators

The flight control surfaces of the high altitude UAV will be actuated by hobby style micro-servos. The autopilot sends commands to the MNAV via an RS-232 serial connection, and the MNAV in turn sends Pulse Width Modulated (PWM) signals to each of the servos (Jang, MNAV Autopilot, 2006). The locations of the servos and their wiring are depicted in Figure 7-5, which shows the planform of the KU Mars airplane design from 2006 (Brown et al., 2006).

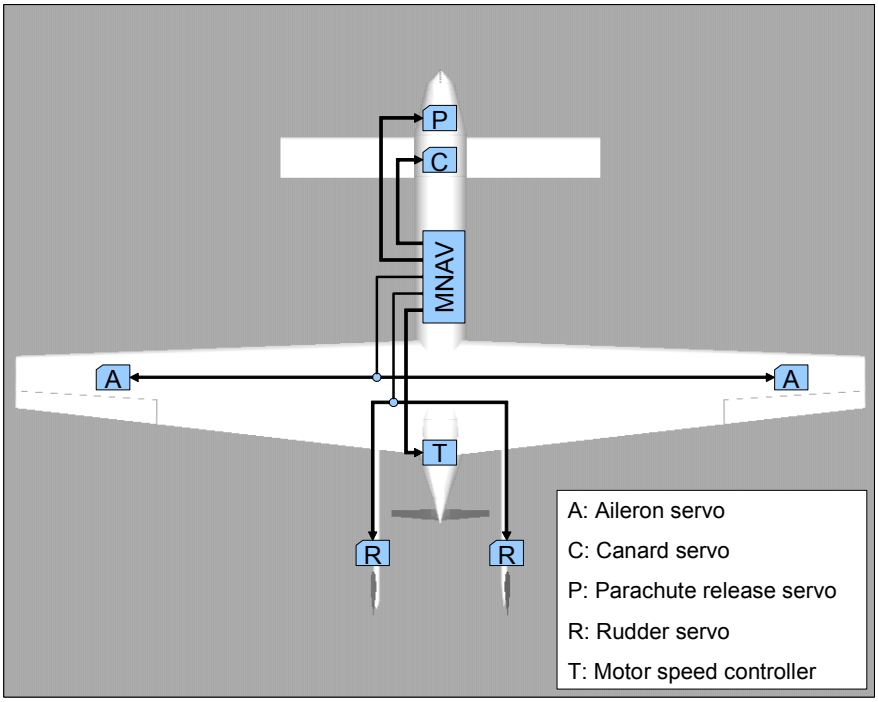

Figure 7-5: Servo Wiring on KU Mars Airplane Design

In addition to flight control surfaces, the high altitude demonstrator will also require actuators for cut-down from the balloon to begin the flight and for releasing the recovery parachute to end the flight. These mechanisms should be driven by so-called "retract

servos," which are commonly used in model aircraft to raise and lower retractable landing gear. The advantages of this type of servo are discussed on page 27.

There remain several important questions about the performance of the servos. Since battery sizing is essential to the success of the high altitude flight test, the servos' power consumption should be tested under a variety of conditions. Depending on the results, power use may have a heavier weight in the design of the autopilot. Vendors claim that analog servos use less energy than newer digital servos; however, no data is readily available that supports or quantifies those claims. There is also the likelihood that energy consumption varies widely between different models of servos or even between different units of the same model type. Power consumption will also likely depend on the age and wear on a particular unit.

Miniature servos for model airplanes also vary widely in responsiveness and accuracy. Very little information is available about the dynamics of this type of actuator, and testing would be useful prior to the design of the control system. Testing should also aim toward identifying nonlinearities in the servo response, such as hysteresis due to gear backlash. These opportunities for future work are reviewed in Section 9.

7.1.5 Ground Station

The high altitude flight test will be facilitated by at least two ground stations. The first ground station will remain stationary at or near the launch site. The second ground station will be inside the XBS chase vehicle, usually a minivan. The personnel in this

vehicle will calculate the landing site of the UAV using the real time telemetry signal to update and revise the predicted location. The balloon team usually uses a second chase vehicle, which provides a platform for a third UAV ground station. It is likely that the UAV will fly beyond the range of the stationary ground station's radio modem. The chase vehicles will follow the UAV to maintain communications. The third ground station would provide redundancy in the event that the link is lost at both of the other stations. The ground station software will run as an application on a ruggedized laptop computer, shown in Figure 7-6. In addition to their physical robustness, these computers also feature bright displays and long battery life suitable for field operations.

Prior to the flight test, each of the ground station computers will be loaded with pertinent geographical data such as highway maps and satellite imagery. The XBS team is equipped with software that overlays telemetry data from the HABS and UAV, as well as the chase vehicle's current location, onto highway maps in near real time (Paruchuri, 2006). The XBS team also uses balloon tracking software capable of combining weather data and current telemetry to produce an accurate prediction of the trajectory (Glahn, 2007), (Paruchuri, 2006).

In addition to the XBS team's tools, the flight test crew will utilize flight data display software that imitates cockpit instruments to display the telemetry data. This software integrates commercial software and custom code developed at the University of Kansas in the related research projects for NASA EPSCoR and CReSIS (Center for the Remote Sensing of Ice Sheets).

Figure 7-6: Ground Station Computer

7.2 Controller Implementation

The aircraft's controller software will run on an onboard embedded computer. The autopilot should be completely autonomous so that the aircraft will continue to operate even if the communications link with the ground station is lost. The single board computer in the current design is the Crossbow Stargate. This computer interfaces directly with the MNAV sensor package and servo controller, as shown in Figure 7-7.

Open-source autopilot software for the Stargate / MNAV solution is available online at http://sourceforge.net/projects/micronav. This software is available at no cost and allows for customization not available from proprietary, closed-source software.

The Stargate supports Compact Flash for data storage. Compact Flash solid state disks

are widely available at low cost, and can accommodate several gigabytes of data. In addition to flight data, it is possible to store images and video on the disk. Storing data locally will provide more information than can be transmitted wirelessly.

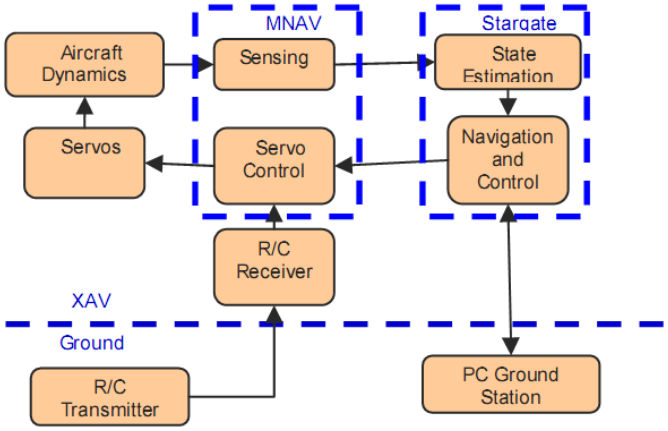

Figure 7-7: Avionics Functional Diagram

(Jang & Liccardo, Inertial Systems, 2006)

The Stargate also supports RS-232 and USB serial connections. The Stargate communicates with the ground station through the wireless modem connected to the RS-232 serial port. The serial port is shown in Figure 7-8.

The autopilot control laws, data acquisition and filtering routines, and other functions are implemented in C code. The software is based on an open-source project hosted by SourceForge (Jang, MNAV Autopilot, 2006). The project Web site does not contain documentation regarding how to implement, operate, or modify the software, but there are extensive forum discussions hosted on the Web site. The forums contain many specific questions and answers posted by software users and contributors. Also, the source code itself contains remarks that partly explain the structure and intended function

of the software. The manufacturer's demonstration of the MNAV and autopilot software is documented in reference (Jang & Liccardo, 2006), which includes a description of the modified Kalman filtering, control loops, and other details. The autopilot software is divided into modules; the modules are summarized in Table 7-1.

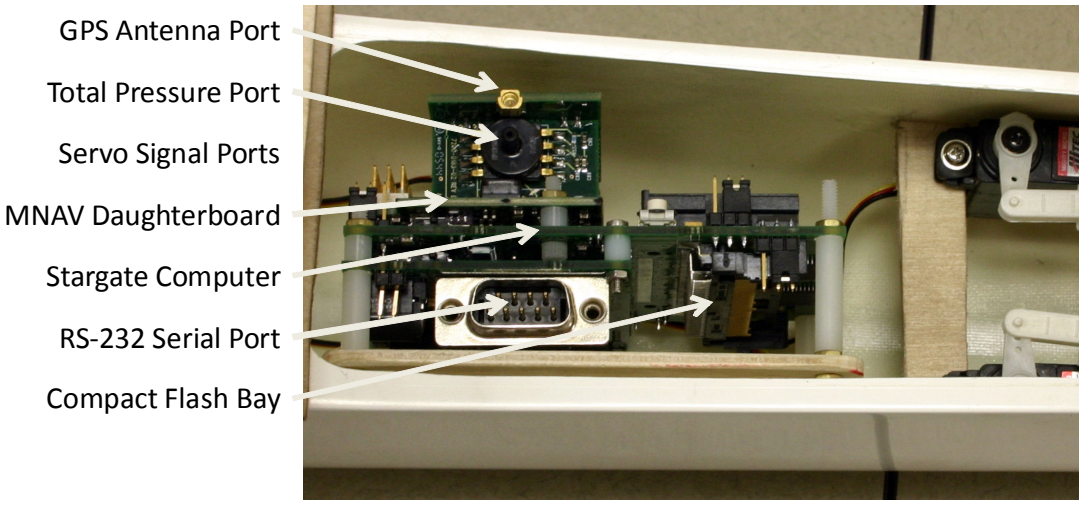

Figure 7-8: Avionics Hardware Installed in Low-Altitude UAV

By default, the MNAV software uses "ncurses" to display the flight data on the console. The programming library "ncurses" allows programmers to design text-based user interfaces that are terminal independent. The avionics application for the MNAV displays a grid of fields that are replaced with the updated live information. However, for the purpose of data logging, it is preferred that each data packet be displayed on a new line, causing the display to scroll. This way, the console display can be streamed across the radio modem link and logged at the ground station without the overhead of the "ncurses" markup codes. The line-by-line format also allows easier parsing later for importing the data into MATLAB. Therefore, the "ncurses" option was turned off for the high altitude communications test flight.

Table 7-1: MNAV Autopilot Software Modules

Filename	Description
ahrs_main.c	Attitude Heading Reference System (AHRS)
	Attitude of the vehicle estimated using an extended Kalman filter
avionics.c	Entry point for autopilot, contains main()
	Parses command line options
	Sets up global variables
	Opens client to transmit and receive packets to and from the ground station by UDP
control.c	Control code
	Obtains the purturbed states
	First order low-pass filter to remove noise
	Outer-loop control: position control
	Outer-loop control: heading and altitude control
	Inner-loop control: pitch and roll attitude control
	Send commands to servos
decoder.c	Used only in post-processing to convert binary flight data logs to ASCII
imugps.c	Opens serial port to sensors device (serial port 2)
	Receives and decodes packets containing GPS, IMU, and servo data
	Gets the time
matrix.c	Functions to create and clear matrices
	Math operations for matrices (matrix addition, determinant, etc.)
misc.c	Miscellaneous functions
navfunc.c	Several navigation functions:
	Converts three Euler rotation angles into direction cosine matrix (DCM)
	Earth Centered, Earth Fixed X, Y, and Z (Ecef) conversion to Latitude, Longitude, and Altitude
	Earth Centered, Earth Fixed (Ecef) conversion to Local East, North, Up (ENU) coordinates
navmain.c	Navigation algorithm
serial.c	Open and configure serial port
uplink.c	Contains initial control gains
	Interprets commands from ground station
	Receives waypoint updates
	Receives gain tuning commands for PID

8 Flight Tests

Different aspects of the high altitude flight test system were evaluated in a series of airborne experiments. Two high altitude balloon flights were conducted in the spring of 2007, followed by a hand-launched flight of the low altitude modified sailplane in the summer. Although the tests were not without problems, they validated key points of the flight test system design and provided useful data points for the next design iteration for a high altitude UAV.

The Experimental Balloon Society (XBS) conducted two high altitude balloon flights in support of the Mars airplane project. The cut-downs from the meteorological balloons were controlled by the High Altitude Balloon System (HABS) module. The HABS also reported position and altitude information via a HF radio link. Two members of the XBS team are licensed radio operators and ensure that the radios operate within FCC regulations.

Abbreviated data from the balloon flights is contained in Appendix A. Detailed accounts of the balloon operations are available in the HABS reports (Sorensen & Stiles, HABS-14 Flight Report, 2006) and (Sorensen & Stiles, HABS-15 Flight Report, 2007).

8.1 Avionics Test

During the development of the avionics system, questions had been raised about potential problems operating electronics at high altitude. A good way to separate the real problems from imagined problems is to conduct a flight test.

8.1.1 Overview

On March 10, 2007, the XBS team launched a 1,500 g balloon carrying the HABS control module, a digital photography and video modules, and a module carrying the sensors and SBC identical to those on the Mars airplane demonstrator. This flight is referred to as HABS-15 and reached an altitude of about 24,400 m (80,000 ft).

Figure 8-1 shows the XBS team members holding the balloon with tethers just before launch. The first chase vehicle was already driving east on Highway K-10 in anticipation of the landing site.

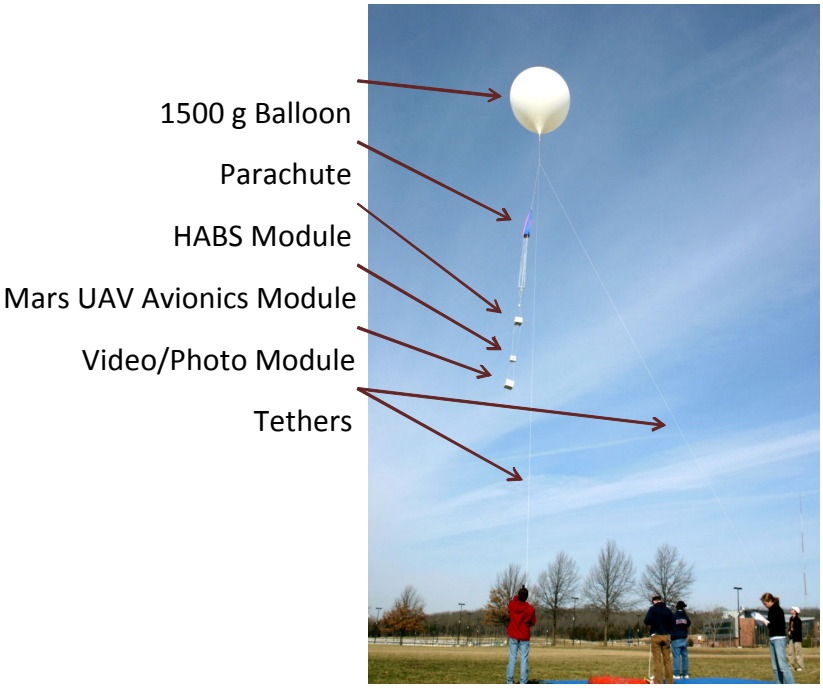

Figure 8-1: HABS-15 Immediately Prior to Launch

The HABS-15 balloon was launched in Lawrence, Kansas near the intersection of 23rd

Street and Iowa Street. The payloads landed just west of Missouri Highway 7 south of 203rd Street. (38° 44' 16" North, 94° 16' 58" West).

Figure 8-2 shows the GPS data recorded by the avionics system. Figure 8-3 shows the telemetry transmitted by the HABS module.

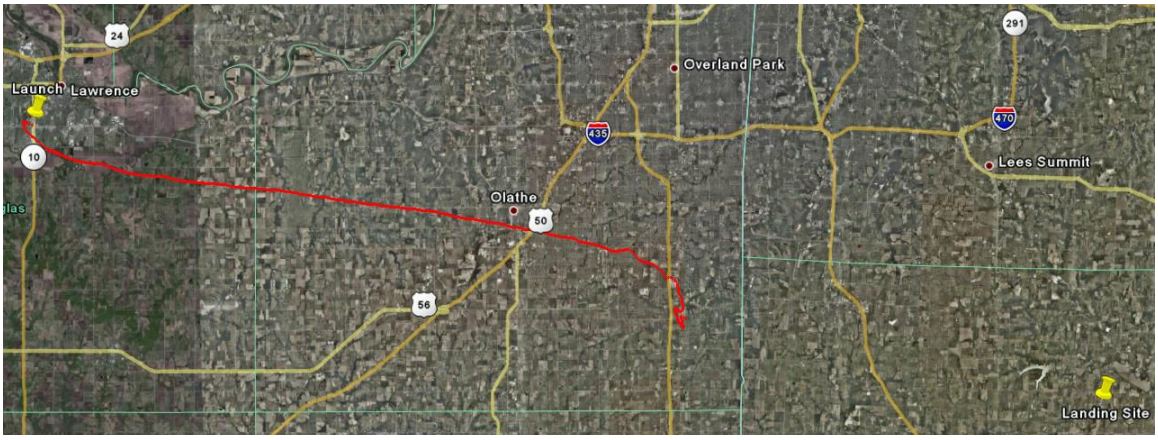

Figure 8-2: HABS-15 Recorded Flight Data

Shortly after the balloon burst, the video from the nadir-facing camera shows that the payloads were tumbling erratically until the parachute opened. Figure 8-4 shows nine video stills from the nadir-facing camera. The first row video frames are from the balloon-lifted ascent and show parts of the university and the neighborhoods of Lawrence, Kansas. The second row images are from immediately after the balloon burst. The payload turned sideways while tumbling and captured the horizon as seen from 23,700 m (78,000 ft). The third row video frames are from the parachute-retarded descent in rural Missouri.

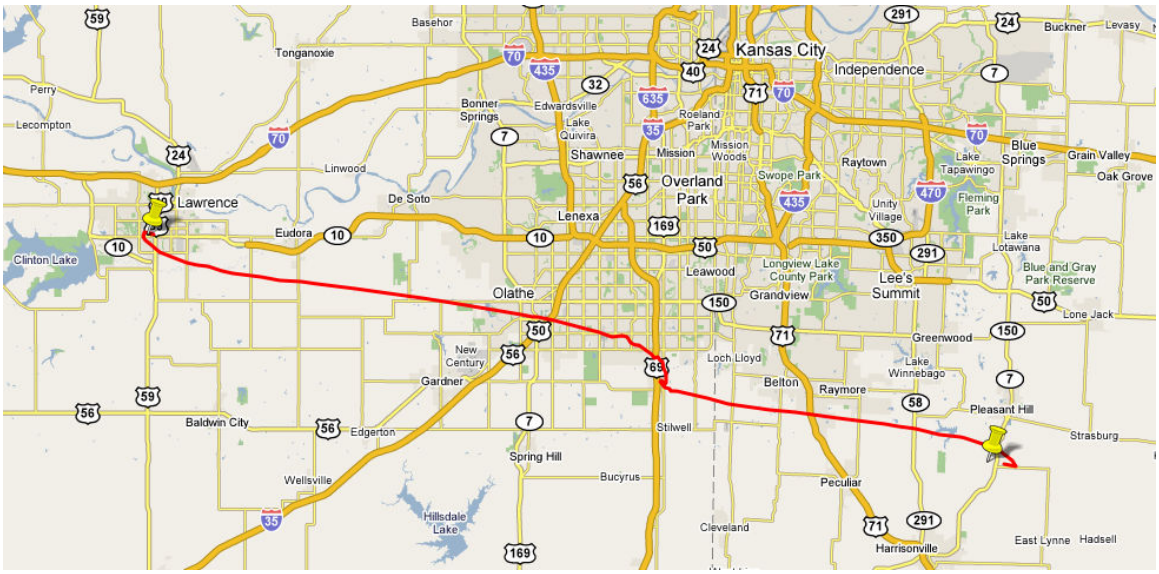

Figure 8-3: HABS-15 Telemetry

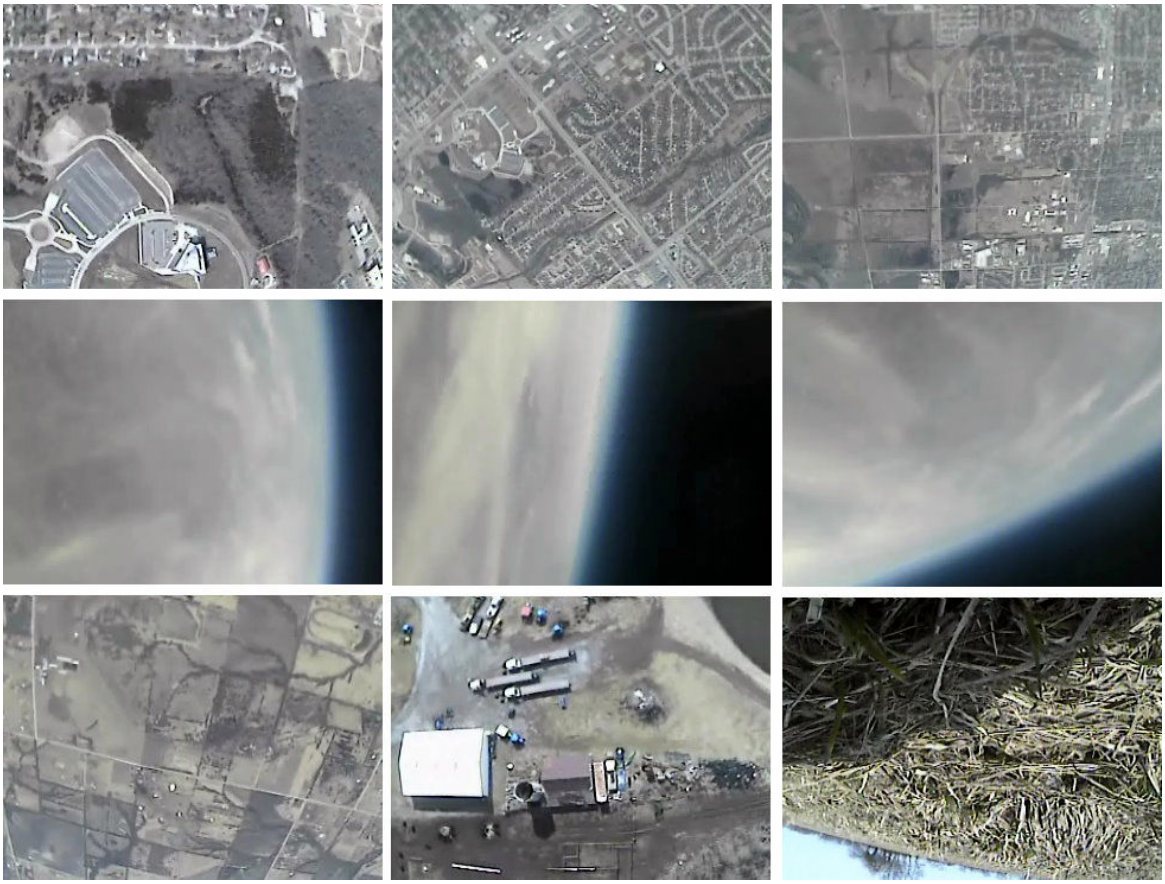

Figure 8-4: Video Stills from Nadir-Facing Camera on HABS-15

8.1.2 Implementation

The avionics box was assembled from pink insulation foam about 25 mm (1 in) thick and wrapped in mylar. The box hung below the HABS module by two cords. The black rubber tubes visible in Figure 8-5 guide the cords through the box. Two chemical hand warmers were activated and inserted into the box before it was shut. After the photograph was taken, the box was sealed with silicone caulk. The battery connection to the avionics was located outside the box so that the power could be disconnected before breaking the seal.

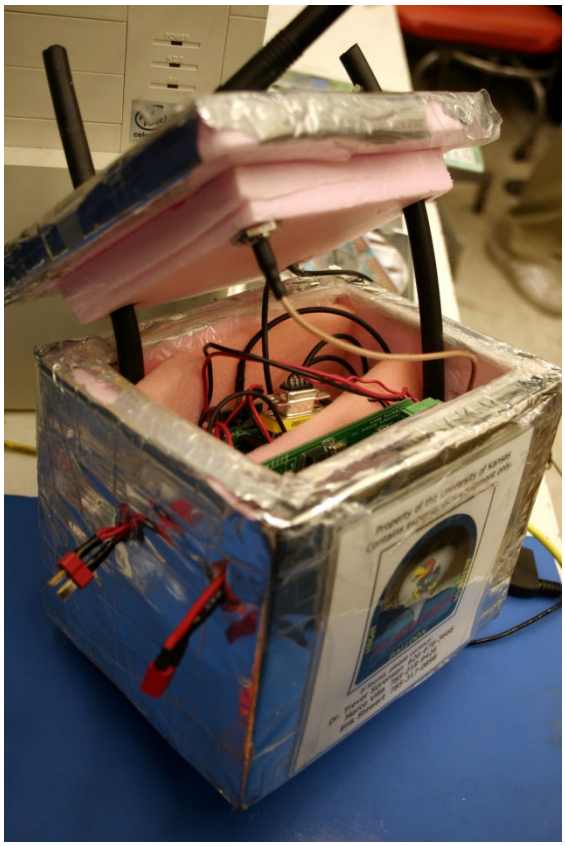

Figure 8-5: Avionics High Altitude Test Module

8.1.3 Results

The payload was recovered, and the binary data stored on the onboard Compact Flash storage was converted to ASCII. The conversion program runs much faster on a desktop computer under Windows XP; however, the output is unreadable. When the conversion program is run on the Stargate single board computer by Linux, the output is readable. It is suspected that the problem is somehow related to endianness, because the Pentium and Xscale processors handle numerical values differently. Endianness describes the byte ordering in memory used to represent data, and care should be taken that the byte order is translated properly for a given system.

Due to a problem with one of the batteries, only one 2,100 mA-hr lithium-polymer battery was used to power the avionics. Since the 3-cell lithium-polymer battery provides 11.1 V, and the Stargate requires less than 8 V, a voltage regulator was added to drop the voltage to 6 V. This type of voltage regulator loses some energy as heat. The limited battery capacity and inefficiency of the voltage regulator contributed to the premature shutdown of the avionics. When the voltage dropped too low, the firmware on the MNAV was corrupted. A utility to reload the firmware on to the MNAV was provided by the manufacturer, Crossbow. The MNAV problem was corrected and the sensors were recalibrated for the next flight. In future missions, the avionics should be shutdown prior to the battery dropping below the minimum voltage requirement. This will require the addition of a circuit that monitors the voltage and sends a signal to the computer when a minimum threshold is reached. Software on the computer shall respond to this signal by commanding an orderly shutdown of the computer, to mitigate data loss.

A separate temperature-logging device called a HOBO was installed in the avionics box to monitor the internal temperature during the flight. The data from the thermistor is plotted in Figure 8-6.

The trend of the temperature inside the insulated avionics box indicates that two hand warmers were capable of keeping the temperature high enough for normal battery performance throughout the high altitude flight test.

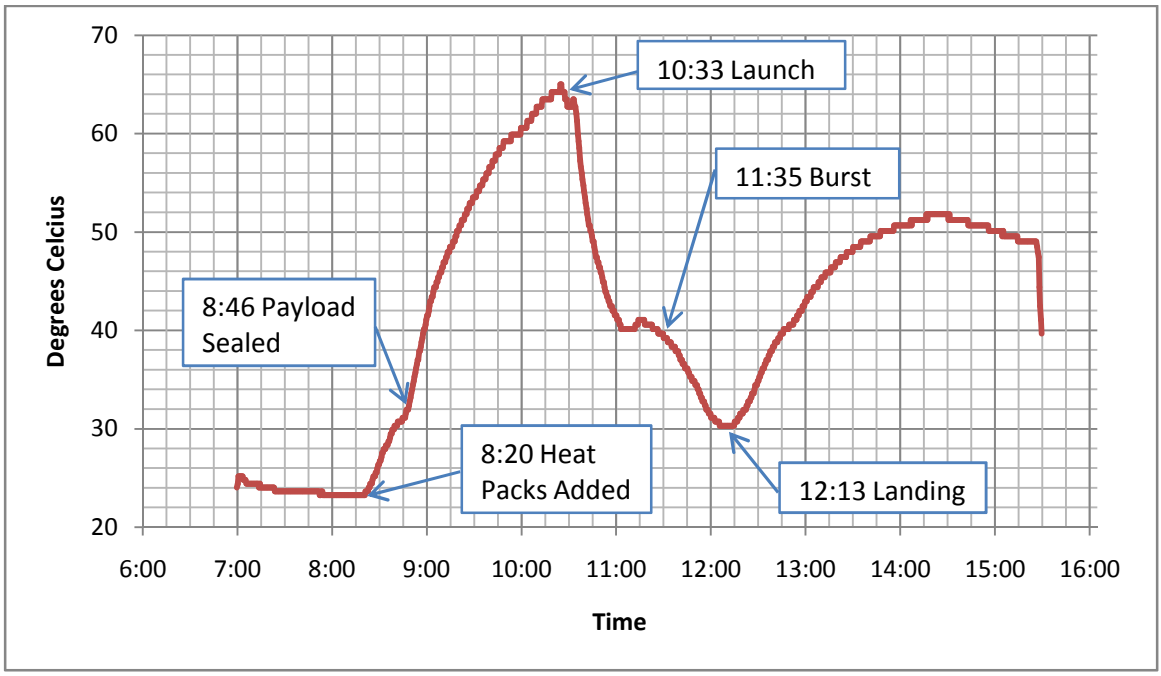

Figure 8-6: Temperature inside Avionics Payload on HABS-15 Flight

8.2 Gust Dynamics & Communications Test

On April 28, 2007, the XBS team launched HABS-16b, a 2,000 g balloon carrying the

HABS control unit, a digital photography and video unit, and a mockup of the Mars airplane, shown in Figure 8-7. The mockup aircraft was a non-flying surrogate made primarily of foam and wooden dowel rods. This model of the Mars airplane had a similar planform to the planned high altitude UAV.

Figure 8-7: Mockup Mars Airplane for High Altitude Testing

At the maximum altitude the ground crew issued the cut-down command to HABS, and the payload modules including the mockup aircraft began tumbling. Around this time, the lines linking the mockup aircraft with the HABS failed, and the aircraft model separated from the other modules. This resulted in an unplanned tumble from high altitude. The telemetry received by the radio modems shows that GPS lock was lost, but inertial data was still being sent. Shortly after that, the communications link was lost. The mockup aircraft and its electronics were lost. The HABS and another module remained connected, parachuted back to the ground, and were recovered by the team.

The HABS sent telemetry data throughout the flight. The ground track is shown in Figure 8-8.

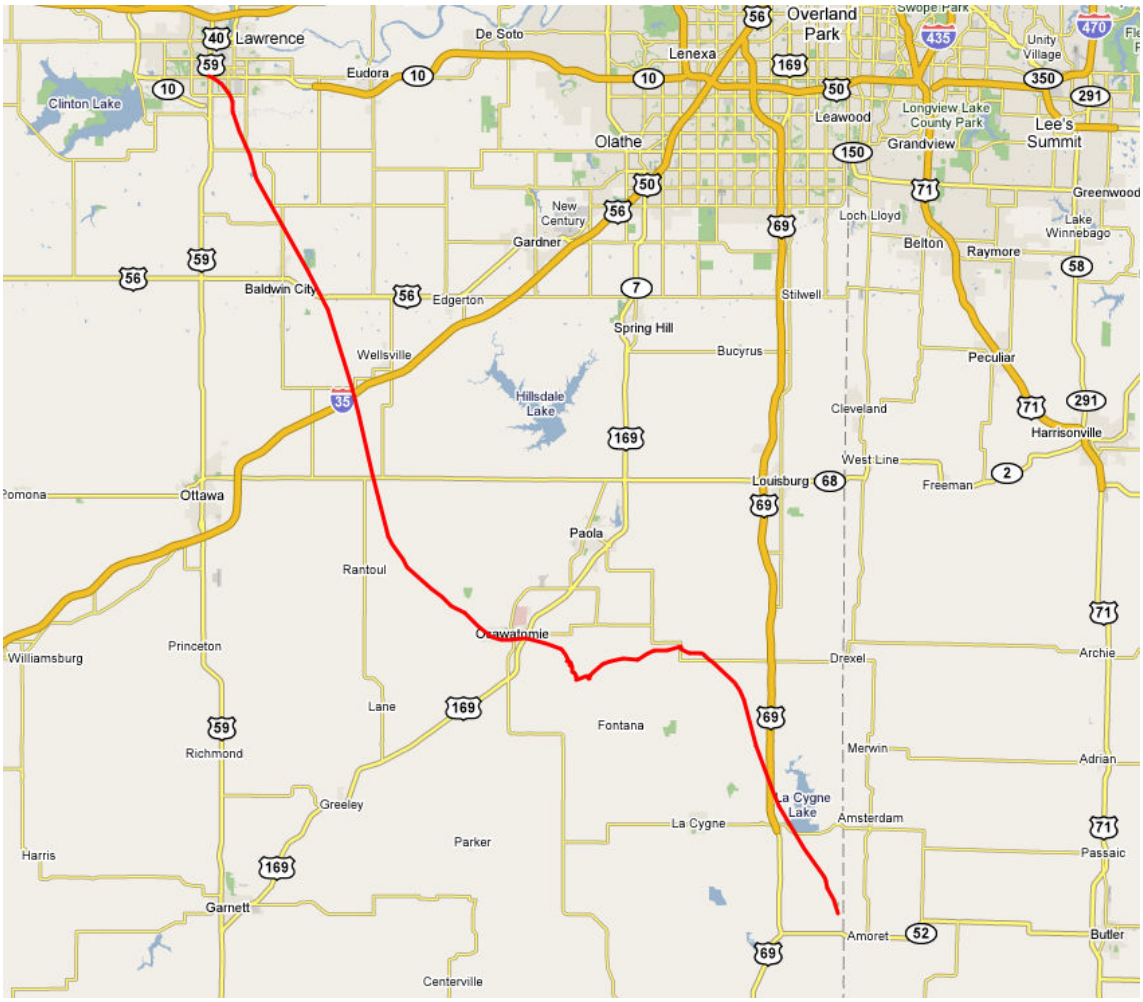

Figure 8-8: HABS-16b Ground Track

Figure 8-9 shows the UAV mock-up being lifted by the balloon. Immediately below the balloon is the folded parachute, and the HABS and photo/video boxes are just above the UAV mock-up.

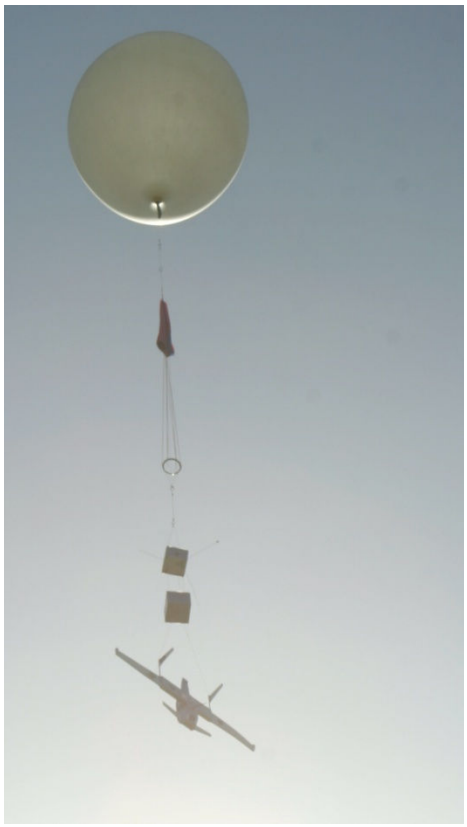

Figure 8-9: HABS-16b Carrying the Mockup UAV

Replacements for the lost avionics components were ordered shortly after they were lost; however, manufacturing delays postponed delivery. As a result, plans for additional avionics testing were deferred.

8.3 Low Altitude Airplane Flight

The low altitude test aircraft was first flown on July 22, 2007, piloted by Dr. David Alexander. The aircraft was modified from a Bird of Time kit in order to accommodate the flight test electronics and an electric motor with folding propeller blades. The goals of the first flight were to give the pilot a feel for the handling of the aircraft and to tune

the high and low gain settings for the ailerons, rudder, and stabilators.

Figure 8-10: Hand Launch of the Low Altitude Test Aircraft

Immediately after launch, the pilot discovered that the stabilators were more effective than anticipated. Although unplanned, his command to pull-up demonstrated significant stabilator control power. When the aircraft is dropped from a balloon a similar maneuver will be required to transition to level flight. The strength of the balsa and thin plastic covering of the wing was sufficient to withstand the high load factor.

Although no instruments were onboard the aircraft, digital video of the flight captured the sudden pull-up. Nine consecutive frames of video have been combined together in Figure 8-11 to illustrate the maneuver. The time step between each frame is 0.0667 sec

or 15 frames per second, so these 9 frames represent about 0.6 sec of video. The images were aligned using background objects such as trees and clouds that did not move substantially relative to the camera position over this brief timescale.

Figure 8-11: Pull-Up Maneuver, Nine Video Frames Overlaid (0.6 sec)

Using software designed for gleaning architectural dimensions from photographs (Google Inc., 2007), an estimated trajectory was constructed by matching the video images of the aircraft to a vertical plane. Figure 8-12 shows how a vertical plane was matched to the video images using the software's Photo Match feature, and a CAD model of the aircraft was used to match the scale of the images. The wingspan and fuselage length of the

aircraft were used to estimate the depth of the composite image. The sailplane model has a 3,000 mm (9.8 ft) wingspan, and the fuselage is 1,360 mm (4.5 ft) long. Note that the wings of the CAD model do not bend to match the images. Figure 8-13 shows the same geometry of the maneuver from a different perspective.

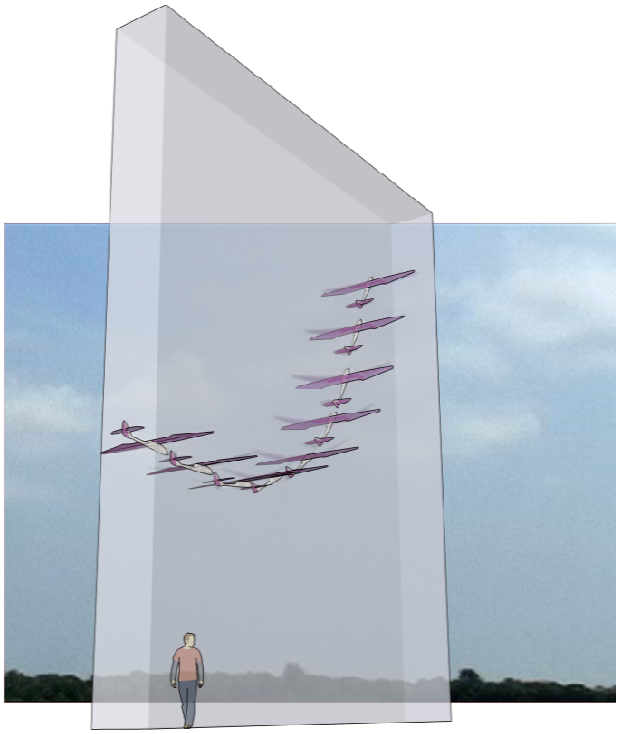

Figure 8-12: Matching Image Perspective with a Vertical Plane

Since the period between frames is about 0.0667 sec, the forward velocity of the UAV is estimated to have been about 20 m/s (39 knots) during this maneuver. The length of the flight path is estimated to have been 12 m (39 ft). The maximum vertical load factor n can be estimated by assuming the pull-up was fixed to a vertical plane, had a constant radius r of 4.8 m (16 ft), and the velocity V was constant at 20 m/s (39 knots).

$$n = \frac{V^2}{r} = 83\,{}^{m}/_{s^2}$$

Therefore, the estimated maximum load factor was about 8.5 G.

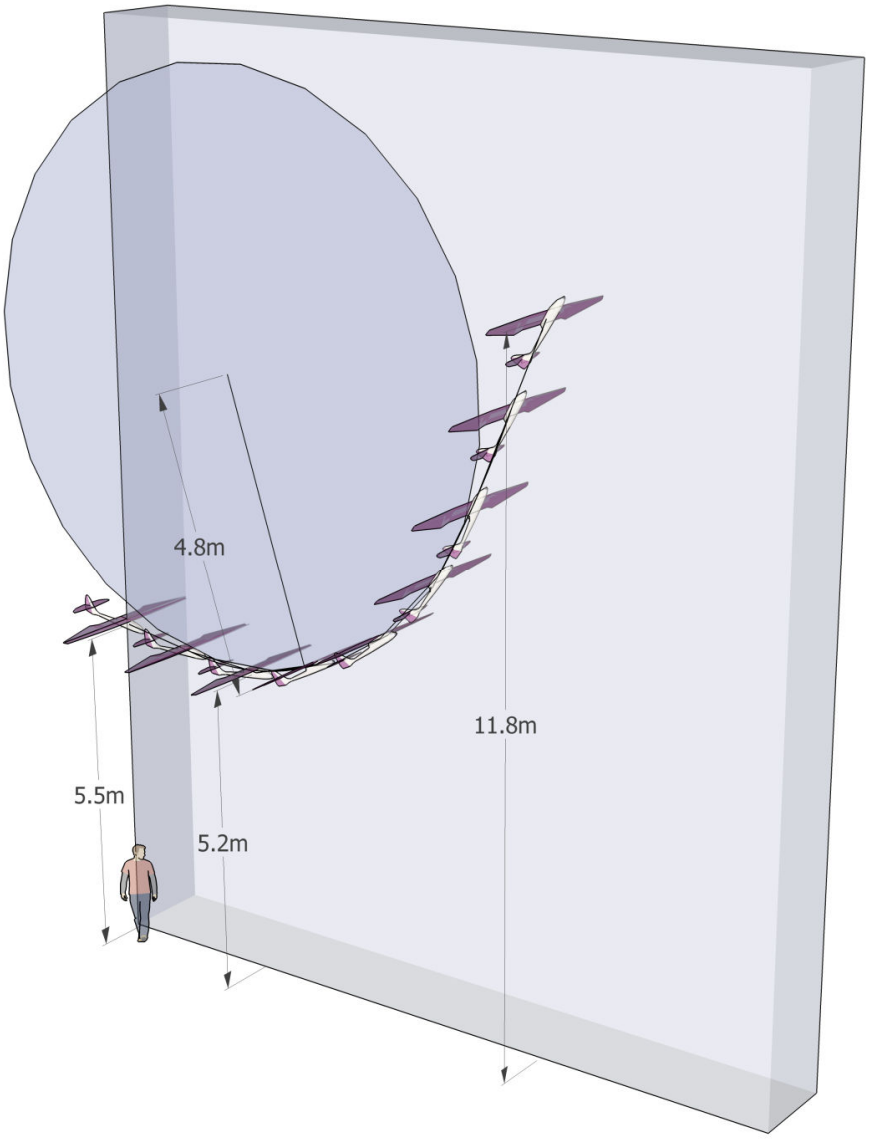

Figure 8-13: Estimated Pull-Up Trajectory

This maneuver demonstrates the robustness of conventional model airplane construction and should give confidence to the designers of the high altitude UAV as they size the spar for the load factor experienced during the transition from balloon ascent to level flight. A single Hitech MG-85 micro servo was used to deflect the stabilators. The pull-up maneuver proved that this servo has adequate torque and speed to manage the variable-incidence stabilator through the balloon-drop and pull-out.

This method of estimating the trajectory using a single video source is imprecise. Errors have likely been introduced due to imperfections in the camera's lens, manual stitching of the composite image, and the lack of geometry information such as the camera's location and focal length. Furthermore, simplifying assumptions were made about the pull-up maneuver. However, given the risk of structural failure, it is unlikely that this maneuver will be repeated with full instrumentation. Therefore, the trajectory estimated here will likely remain the best-available data in preparation for the balloon-drop maneuver.

After the flight, the pilot made recommendations to improve the handling qualities of the low altitude test aircraft. The pilot commented that the roll response was poor, and suggested increasing the gains to the ailerons if possible. Alternatively, he suggested mixing in 50% of rudder with full aileron deflection. He also commented that the stabilator gains were set too high. The incidence angles of the stabilators were estimated to be from -15 to 15 deg as called for by the aircraft designer, but should be more precisely measured before future flights. The pilot also noted that the c.g. may have been too far aft, but it was difficult to be certain because of the high control power of the

stabilators. Finally, the pilot said the aircraft was prone to tip-stalls, which is also evident in the video on at least two occasions.

The flight ended unexpectedly due to tip stall. The pilot was able to partially recover from the stall just before impact, so the only damage to the aircraft was a crack in the motor mount. The damage is easily repairable.

Prior to launch, the current draw of the motor was tested at high throttle. With a 14x9 propeller, the motor was drawing more amps than recommended by the manufacturer. Therefore, an upper limit was set on the throttle to prevent drawing too much current during the flight. In future flights, a smaller propeller should be used.

Additional flights of the low altitude UAV will be helpful in the integration of the avionics systems in an airborne test bed. Future flight testing will include dropping the UAV from a tethered balloon, so that the balloon can be reused for multiple iterations of the flight test.

9 Recommendations for Future Work

A number of interesting research possibilities related to flight testing of UAVs at high altitude were uncovered during the development of this design. Some of this work should be done prior to the high altitude flight test.

It is recommended that the Mars airplane design be revised. Particular attention should be given to the selection of the electric motor and the propeller. Based on the significant climb performance of the low altitude UAV, the motor is more powerful than necessary. It is believed that the motor selected for the high altitude UAV is also over-powered. Note that the balloon-dropped airplanes will only need power to maintain altitude and do not need to be sized for climbing or other maneuvers. By reducing the motor size, weight and energy savings can be gained.

Research by Colozza and others shows that propeller design for low Reynolds number conditions will be challenging due to a lack of data. Since electric motors can easily be used inside wind tunnels, there is an opportunity to acquire very useful empirical data about propeller performance in low Reynolds number flows. It is recommended that a variety of commercially available propellers and custom designed propellers should be tested in the wind tunnel. The motor should be instrumented to record thrust, current draw, rotation rate, and temperature. If possible, hot film instruments could be attached to the trailing edges of the propellers, as proposed by Colozza (Colozza, APEX 3D Propeller Test Preliminary Design, Sept. 2002).

Wind tunnel testing could also find downwash angles on stabilators, or interference between the canard and wing in the KU high altitude UAV design. These interactions are difficult to predict analytically, and the process is complicated by issues related to low Reynolds number flows.

It is recommended that significant testing be invested in the parachute deployment system. Testing will help revise the high altitude UAV design so that the recovery system is more reliable and robust.

When the Mars airplane demonstrator is constructed, the moment of inertia of each major axis should be measured using the three string torsional pendulum method described in Section 4.1. Accurate measurements of the moments of inertia will lead to better dynamic model of the aircraft for simulation and controller design.

It is recommended that software tools be evaluated regarding their validity in low Reynolds number flows. Many software packages rely on trends in empirical data, which has mostly been collected by crewed airplanes flying only over the Earth. The data produced by this flight test should be useful for checking the validity of the software predictions of the aircraft's flight characteristics within low Reynolds number conditions.

It is recommended that a system be developed that logs the actual deflection of the flight critical control surfaces. The positions of deflected ailerons, elevators, and rudders should be measured with potentiometers and stored with the other flight test data. These measurements should be made on the low altitude avionics testbed UAV as well as on the

final Mars airplane demonstrator.

As the high altitude UAV design is revised and finalized, a nonlinear model should be developed and a robust controller should be synthesized using methods described by Colgren (Colgren, 2004).

The communications code for the Stargate should be modified to suit the radio modem. The current software is designed for the 802.11b wireless networking protocol. Some unnecessary characters can be removed from the data stream to make it more efficient. Also, the code should be modified for two data rate modes. The first mode should be a high data rate for use during the flight test maneuvers portion of the flight. The second mode should reduce the data rate in order to conserve battery power during the ascent and descent phases of the flight.

A number of thin-film solar cells were purchased for testing as a source of energy onboard the high altitude UAV. A circuit capable of recharging the lithium-polymer avionics battery should be designed so that the photovoltaic energy supplements the battery life of the avionics. The flexible solar cells are 0.2 mm thick and are already prepared with a pressure sensitive adhesive. To install a cell, the plastic backing must be removed from the cell. The photovoltaic material is laminated with thin clear plastic. The plastic covering the copper leads must be melted with a soldering iron or cut away with a blade prior to soldering wires to the cell.

The radio modem module should be more directly integrated with the avionics hardware.

Currently, the modem module resides in a developers board that draws additional power. Connecting TTL signals between the Stargate and the radio modem should reduce weight and power consumption.

The flight test team should consider designing the high altitude UAV such that HABS is not required. This simplifies the task of the chase vehicles, since they would only need to recover one object. The UAV must be able to actuate the cut-down mechanism. It is probably best to use a retract servo to release the string, especially when compared to the heat-coil method used by XBS.

10 Conclusions and Recommendations

The hardware and software integrated and tested so far show that the high altitude flight test of a UAV at KU is feasible and would be meaningful to designers of Mars airplanes as well as designers of MAVs. One of the biggest concerns of the KU Mars airplane design team was the transition to normal flight after the balloon cut-down. Simulations and related research indicate that the transition maneuver is feasible. Also, low altitude flight tests demonstrated significant stabilator control power and structural robustness. The inadvertent pull-up maneuver also demonstrated that micro servos have sufficient torque to deflect the variable incidence stabilators to large negative angles.

Testing of the telemetry communications system has shown that the range is sufficient to support the high altitude flight test. Other high altitude flights proved that the proposed thermal management system is sufficient to maintain the temperatures required for the batteries and electronics to function. The testbed aircraft is ready for additional flight tests to support the development of the autopilot and for the testing of parachute deployment.

A more conventional aircraft configuration, with stabilators rather than canards, should be used for Mars exploration and high altitude flight testing. Relatively similar conventional configurations have been wind tunnel and flight tested in similar Reynolds number flows, including the modified sailplane utilized in this project for low altitude flights. Also, a sailplane configuration was flight tested by NASA in controlled deep stalls. Dropping the aircraft from the balloon in a deep stall attitude may be an effective

method to prevent losing altitude after the separation. Also, entering a controlled deep stall, combined with airbags, is a realistic way to land an aircraft on the Martian surface.

As development of the Mars exploration aircraft continues, researchers should utilize the sources listed in the Bibliography. These sources contain many lessons learned as well as data that will aid in the analysis of revised designs.

It is recommended that the high altitude flight test team collaborate with the Experimental Balloon Society (XBS). As the team prepares for the flight test, is it vitally important that the operation be planned and rehearsed well in advance of the launch date.

The Mars UAV demonstrator team should continue the relationship with EaglePicher and Lockheed Martin. These partners can contribute experience and resources that will significantly enhance the progress of the project.

Much of that data and multimedia generated during this research is collected in computer files. These files are available on CD-ROM or DVD-ROM from the author. The data, photos, and video in this collection will likely be useful in the continued development of high altitude UAVs and related flight testing.

Bibliography

Anderson, J. D. (1997). *A History of Aerodynamics and Its Impact on Flying Machines.* New York: Cambridge University Press.

Anderson, J. D. (2001). *Fundamentals of Aerodynamics* (3rd Ed. ed.). New York: McGraw-Hill.

Anderson, J. D. (2005). *Introduction to Flight, 5th ed.* New York: McGraw Hill.

ARES - A Proposed Mars Scout Mission. (17 January 2007). Retrieved 2 July 2007, from http://marsairplane.larc.nasa.gov

Brion, V., Aki, M., & Shkarayev, S. (2006). Numerical Simulations of Low Reynolds Number Flows Around Micro Air Vehicles and Comparison against Wind Tunnel Data. *24th Applied Aerodynamics Conference, 5-8 June 2006.* San Francisco, CA: AIAA 2006-3864.

Brown, Dhruv, Oh, Hupe, Landavazo, Pasupuleti, et al. (2006). *Design of a Stability, Control, and Performance Demonstrator of a Mars Airplane.* Lawrence, KS: University of Kansas.

Carr, M. H. (2007). *The Surface of Mars.* New York: Cambridge University Press.

Colgren, R. (2004). *Applications of Robust Control to Nonlinear Systems.* AIAA.

Colgren, R. D., & Martin, K. E. Flight Test Validation of Sideslip Estimation Using Inertial Accelerations. *Guidance, Navigation, and Control Conference and Exhibit, 14-17 August 2000.* Denver, CO: AIAA 2000-4448.

Colozza, A. J. (Sept. 2002). *APEX 3D Propeller Test Preliminary Design.* NASA, CR-2002-211866.

Colozza, A. J. (April 1990). *Preliminary Design of a Long-Endurance Mars Aircraft.* NASA, CR 185243.

Crossbow Technology, Inc. (2006). *Inertial Systems.* Retrieved April 2007, from Crossbow: http://www.xbow.com/Products/Product_pdf_files/Inertial_pdf/uNAV_Datasheet.pdf

DARcorporation. (2006). *Advanced Aircraft Analysis (AAA) Ver. 3.1.* Lawrence, KS.

Dogan, A., & Kabamba, P. T. Escaping Microburst with Turbulence: Altitude, Dive, and Pitch Guidance Strategies. *Journal of Aircraft, Vol. 37, No. 3, May–June 2000.* AIAA 2642-172.

Foster, T. M., & Bowman, W. J. Dynamic Stability and Handling Qualities of Small Unmanned-Aerial-Vehicles. *43rd AIAA Aerospace Sciences Meeting and Exhibit, 10-13 January 2005.* Reno, NV: AIAA 2005-1023.

Glahn, R. v. (17 April 2007). Retrieved 15 June 2007, from Balloon Track for Windows: http://www.eoss.org/wbaltrak/

Google Inc. (2007). *Google SketchUp ver. 6.0.515.* Retrieved from Google SketchUp Home: http://sketchup.google.com

GPO Access. (11 July 2007). (National Archives and Records Administration) Retrieved 13 July 2007, from Electronic Code of Federal Regulations (e-CFR): http://ecfr.gpoaccess.gov

Greer, D., Hamory, P., Krake, K., & Drela, M. (1999). *Design and Predictions for a High-Altitude (Low-Reynolds-Number) Aerodynamic Flight Experiment.* Edwards, CA: NASA, TM-1999-206579.

Guynn, M. D., Croom, M. A., Smith, S. C., Parks, R. W., & Gelhausen, P. A. (2003). Evolution of a Mars Airplane Concept for the ARES Mars Scout Mission. *2nd AIAA "Unmanned Unlimited" Systems, Technologies, and Operations, 15-18 September 2003.* San Diego, CA: AIAA 2003-6578.

Hall, D. W., Parks, R. W., & Morris, D. S. (1997). *Airplane for Mars Exploration: Conceptual Design of the Full-Scale Vehicle Design, Construction and Test of Performance and Deployment Models.* Sunnyvale, CA: David Hall Consulting.

Hall, J., Lawrence, D., & Mohseni, K. Lateral Control and Observation of a Micro Aerial Vehicle. *45th AIAA Aerospace Sciences Meeting and Exhibit, 8-11 January 2007.* Reno, NV: AIAA 2007-663.

Hoak, D., & Fink, R. (1979). *The USAF Stability and Control Digital DATCOM.* Air Force Flight Dynamics Laboratory: USAF, AFFDL-TR-79-3032.

How, J. (2003). *Aerospace Engineering 16.61 Aerospace Dynamics Lecture Notes.* Retrieved May 2007, from MIT OpenCourseWare: http://ocw.mit.edu

Huber, J., & Sarigul-Klijn, N. In-Flight Reconfigurable Autopilot for Unmanned Aircraft: Hardware Development and Flight Test Results. *Atmospheric Flight Mechanics Conference and Exhibit, 21-24 August 2006.* Keystone, CO: AIAA 2006-6507.

Iliff, K. W. (1989). Parameter Estimation for Flight Vehicles. *J. Guidance* , Sept.-Oct. 1989, Vol. 12, No. 5. AIAA 20454-382.

Jang, J. S. (October 16 2006). *MNAV Autopilot*. Retrieved 1 July 2007, from SourceForge: http://sourceforge.net/projects/micronav

Jang, J. S., & Liccardo, D. (October 15 2006). *Inertial Systems.* Retrieved May 2007, from Crossbow: http://www.xbow.com/General_Info/Info_pdf_files/MNAV_App_Note.pdf

Jodeh, N. M., Blue, P. A., & Waldron, A. A. (2006). Development of Small Unmanned Aerial Vehicle Research Platform: Modeling and Simulating with Flight Test Validation. *Modeling and Simulation Technologies Conference and Exhibit, 21-24 August 2006.* Keystone, CO: AIAA 2006-6261.

Jung, D., & Tsiotras, P. Inertial Attitude and Position Reference System Development for a Small UAV. *Infotech@Aerospace Conference and Exhibit, 7-10 May 2007.* Rohnert Park, CA: AIAA 2007-2763.

Jung, D., & Tsiotras, P. Modeling and Hardware-in-the-Loop Simulation for a Small Unmanned Aerial Vehicle. *Infotech@Aerospace Conference and Exhibit, 7-10 May 2007.* Rohnert Park, CA: AIAA 2007-2768.

Kingston, D., Beard, R., McLain, T., Larsen, M., & Ren, W. Autonomous Vehicle Technologies for Small Fixed Wing UAVs. *2nd AIAA "Unmanned Unlimited" Systems, Technologies, and Operations, 15-18 September 2003.* San Diego, CA: AIAA 2003-6559.

Krashanitsa, R., Platanitis, G., Silin, B., & Shkarayev, S. (2006). Aerodynamics and Controls Design for Autonomous Micro Air Vehicles. *Atmospheric Flight Mechanics Conference and Exhibit, 21-24 August 2006.* Keystone, CO: AIAA 2006-6639.

Lafontaine, J., Lévesque, J.-F., & Kron, A. Robust Guidance and Control Algorithms using Constant Flight Path Angle for Precision Landing on Mars. *Guidance, Navigation, and Control Conference and Exhibit, 21-24 August 2006.* Keystone, CO: AIAA 2006-6075.

Laminar Research. (2007). *About X-Plane.* Retrieved November 2006, from X-Plane by Laminar Research: http://www.x-plane.com/about.html

Lee, C. S., Pang, W. W., Srigrarom, S., Wang, D.-B., & Hsiao, F.-B. (2006). Classification of Airfoils by Abnormal Behavior of Lift Curves at Low Reynolds Number. *24th Applied Aerodynamics Conference.* San Francisco, California: AIAA 2006-3179.

Lee, S., Bjarke, L., Greer, Tatineni, Zhong, & Jacobson. (March 25-26, 1998). *APEX Critical Design Review.* Edwards, CA: NASA Dryden Flight Research Center.

Levine, J. S., Blaney, D. L., Connerney, J. E., Greeley, R., Head, J. W., Hoffman, J. H., et al. (2003). Science from a Mars Airplane: The Aerial Regional-Scale Environmental Survey (ARES) of Mars. *2nd AIAA "Unmanned Unlimited" Systems, Technologies, and Operations, 15-18 September 2003.* San Diego, CA: AIAA 2003-6576.

Mahdavi, F. A., & Sandlin, D. R. (1984). *Flight Determination of the Aerodynamic Stability and Control Characteristics of the NASA SGS 1-36 Sailplane in the Conventional and Deep Stall Angles-of-Attack of between -5 and 75 Degrees.* San Luis Obispo, CA: NASA, CR-176962.

Marchman, J. F. (1987). Aerodynamic Testing at Low Reynolds Numbers. *J. Aircraft* , Feb. 1987, Vol. 24, No. 2. AIAA 45426-771.

Marchman, J. F., & Werme, T. D. (1984). Clark-Y Airfoil Performance at Low Reynolds Numbers. AIAA.

MATLAB and Simulink. (1994-2007). Natick, MA: The MathWorks, Inc.

Melin, T. (2001). *Tornado Ver. 1.0, Release 2.3.* Stockholm, Sweden: Royal Institute of Technology (KTH).

Microhard Systems Inc. (2007). Retrieved November 2006, from Microhard Systems Inc.: http://www.microhardcorp.com

Murray, J., Moes, T., Norlin, K., Bauer, J., Geenen, R., Moulton, B., et al. (1992). *Piloted Simulation Study of a Balloon-Assisted Deployment of an Aircraft at High Altitude.* Edwards, CA: NASA, TM-104245.

NASA Photo: ECN-26847. (1983). Retrieved 11 July 2007, from NASA Dryden Flight Research Center Photo Collection: http://www.dfrc.nasa.gov/gallery/photo/index.html

Omega Engineering Inc. (2006). *Products.* Retrieved November 2006, from omega.com: www.omega.com

Paruchuri, N. (2006). *The HABS, KUBESat, KUTESat KUTESat-1 Technical report; Design of a Modular platform for Picosatellites.* Lawrence, KS: University of Kansas.

Past Projects - APEX. (July 19 2006). (NASA) Retrieved 8 May 2007, from Frequently Asked Questions: http://www.nasa.gov/centers/dryden/history/pastprojects/Apex/apexlist.html

Platanitis, G., & Shkarayev, S. (2005). Integration of an Autopilot for a Micro Air Vehicle. *Infotech@Aerospace, 26-29 September 2005.* Arlington, VA: AIAA 2005-7066.

Raymer, D. P. (1999). In J. S. Przemieniecki (Ed.), *Aircraft Design: A Conceptual Approach* (3rd Edition ed.). Reston, VA: AIAA.

Re, R. J., Odis C. Pendergraft, J., & Campbell, R. L. (2006). *Low Reynolds Number Aerodynamic Characteristics of Several Airplane Configurations Designed to Fly in the Mars Atmosphere at Subsonic Speeds.* Hampton, VA: NASA, TM-2006-214312.

Reasor, D. A., LeBeau, R. P., Smith, S. W., & Jacob, J. D. Flight Testing and Simulation of a Mars Aircraft Design Using Inflatable Wings. *45th AIAA Aerospace Sciences Meeting and Exhibit, 8-11 January 2007.* Reno, NV: AIAA 2007-0243.

Roskam, J. (1991). *Airplane Design Part VII : Determination of Stability Control and Performance Characteristics: FAR and Military Requirements.* Lawrence, KS: DARcorporation.

Sadraey, M., & Colgren, R. Robust Nonlinear Controller Design for a Complete UAV Mission. *Guidance, Navigation, and Control Conference and Exhibit, 21-24 August 2006.* Keystone, CO: AIAA 2006-6687.

Selig, M. S., & Guglielmo, J. J. (1997). High-Lift Low Reynolds Number Airfoil Design. *Journal of Aircraft* , Jan.-Feb. 1997, Vol. 34, No. 1. AIAA 2137-229.

Sim, A. G. (1984). *Flight Characteristics of a Manned, Low-Speed, Controlled Deep Stall Vehicle.* Edwards, CA: NASA Dryden Flight Research Center.

Sorensen, T. C., Villa, M., & Brown, K. D. The Kansas Universities' Technology Evaluation Satellite Program. *Space 2005, 30 Aug.-1 Sept. 2005.* Long Beach, CA: AIAA 2005-6793.

Sorensen, T., & Stiles, L. (2006). *HABS-14 Flight Report.* Lawrence, KS: University of Kansas.

Sorensen, T., & Stiles, L. (2007). *HABS-15 Flight Report.* Lawrence, KS: University of Kansas.

U.S. Standard Atmosphere. (1976). Washington, D.C.: U.S. Government Printing Office.

Victor C. Clarke, J., Keren, A., & Lewis, R. (1979). *A Mars Airplane... Oh Really?* AIAA.

Wagner, E. R., & Cooney, C. E. (1979). *Universal Joint and Driveshaft Design Manual.* SAE.

Wahlers, K. E. (May 2006). *A Design for a High Altitude Flight Test System.* Mississippi: Masters Thesis, Mississippi State University.

Appendix A.

Balloon Flight Data

Details of the HABS 15 flight are reported in the Flight Report included on the DVD-ROM.

March 10, 2007: Flight Summary

Balloon: Kaymont 1,500 g sounding balloon, inflated to 18.5 pounds lift

Launch: 10:33 CDT on March 10th, 2007 from the 23rd and Clinton Parkway soccer fields (38.94378º N, 95.2621º W, 886 ft).

Burst: 11:35 CDT

Max Altitude: 78,024 ft

Landing: South of Pleasant Hills, Missouri (38.736º N, 94.271º W) at 12:13 CDT

Total Time of Flight: 103 minutes (61 minutes ascent, 42 minutes descent)

Average Ascent Rate: 1,161 ft /min

Average Descent Rate: 2,030 ft /min

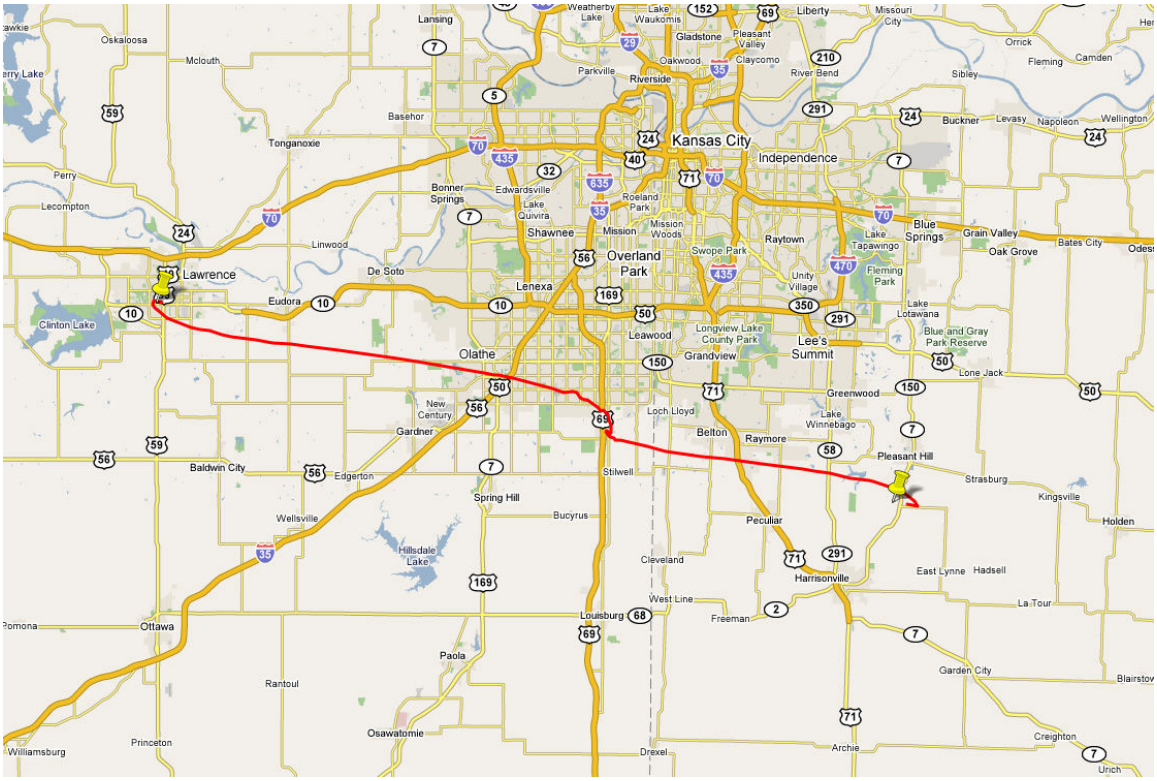

Figure A-1: Ground Track of HABS-15

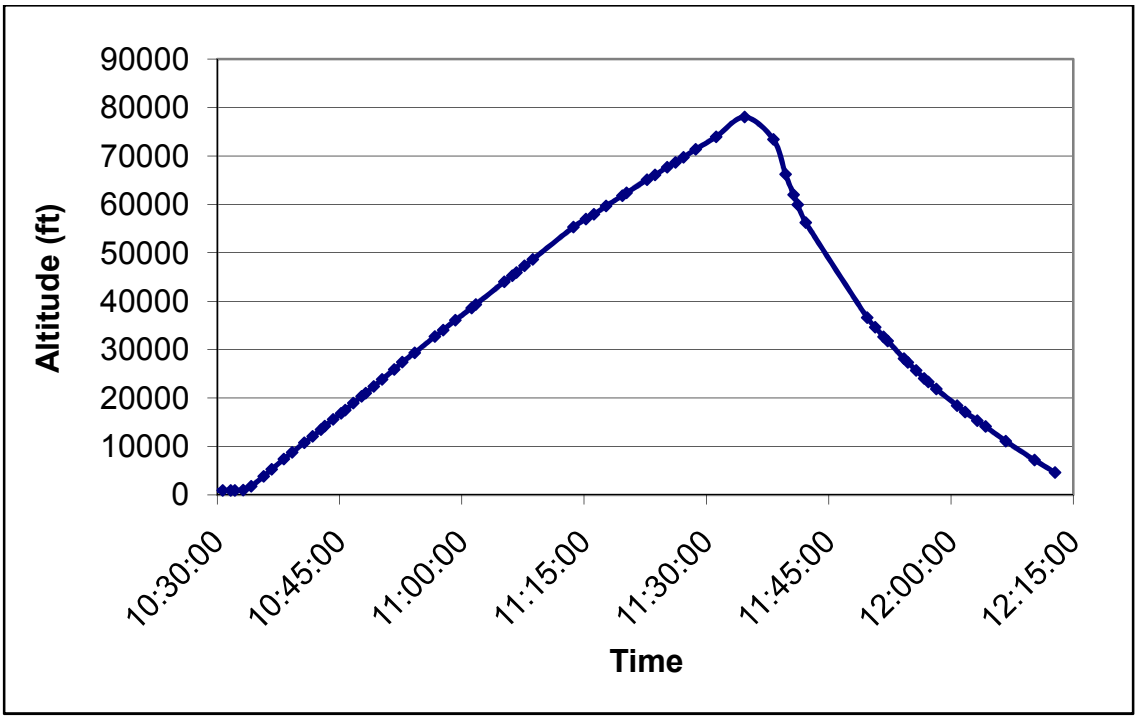

Figure A-2: HABS 15 Altitude Profile

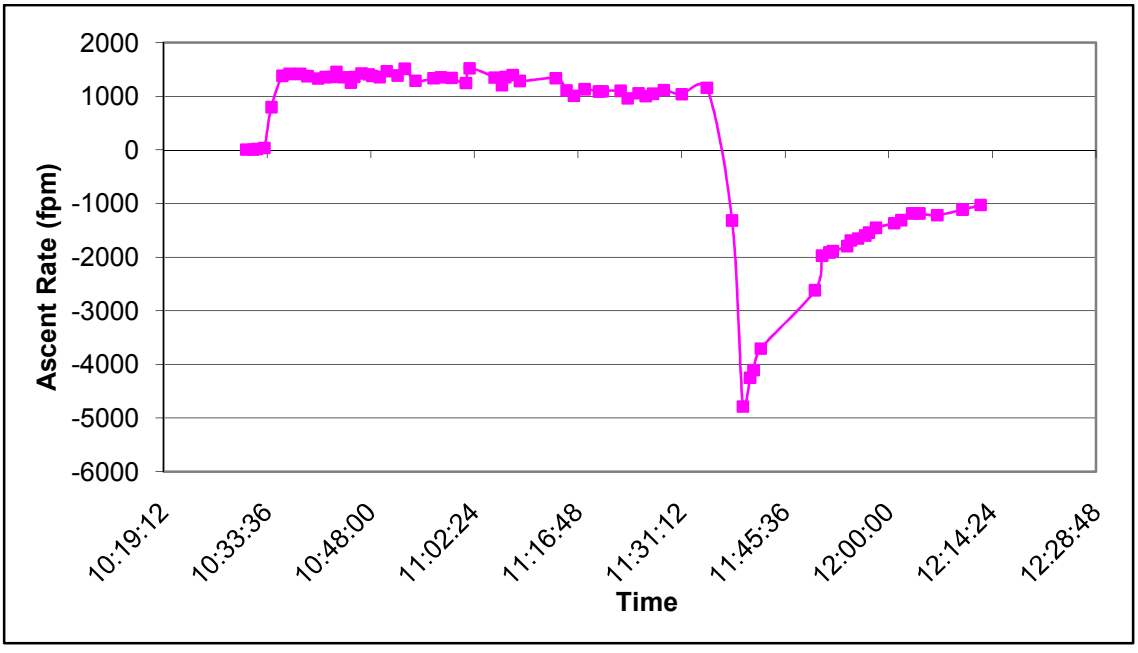

Figure A-3: HABS 15 Ascent Rate

April 28, 2007: Flight Summary

No Flight Report for HABS-16b was available. The following map shows the flight path.

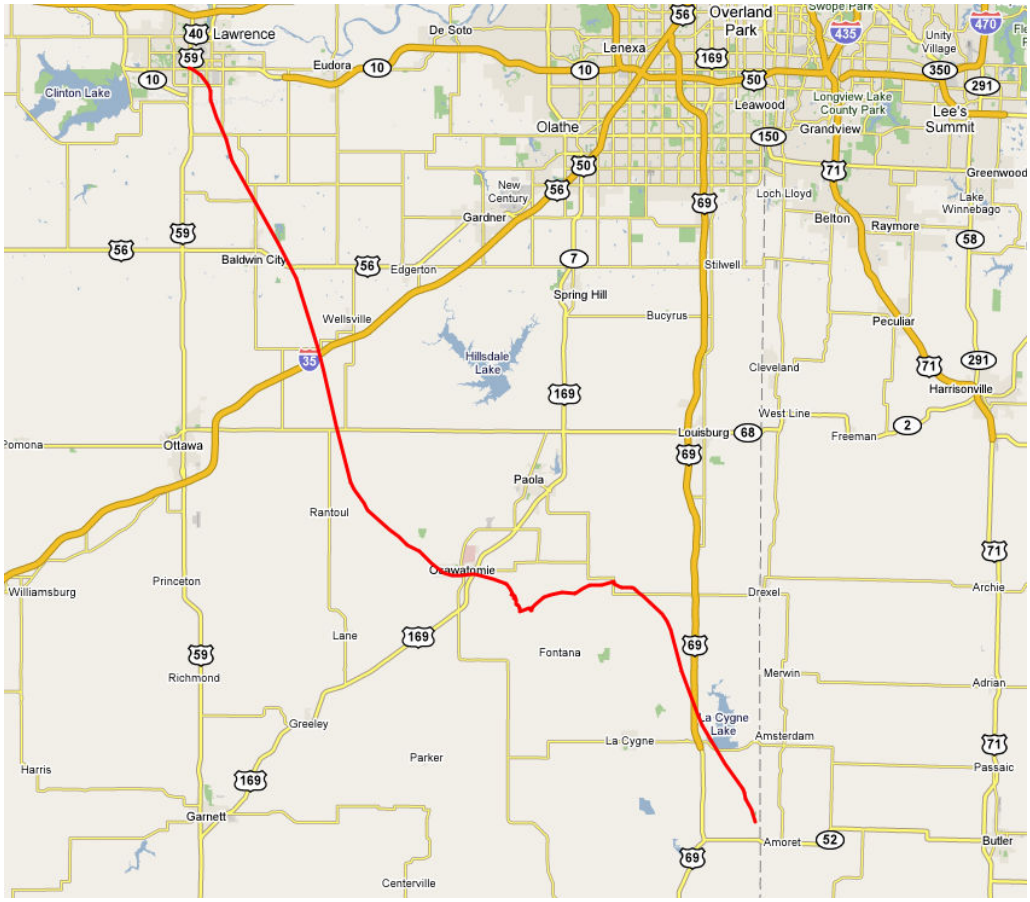

Figure A-4: Ground Track of HABS-16b

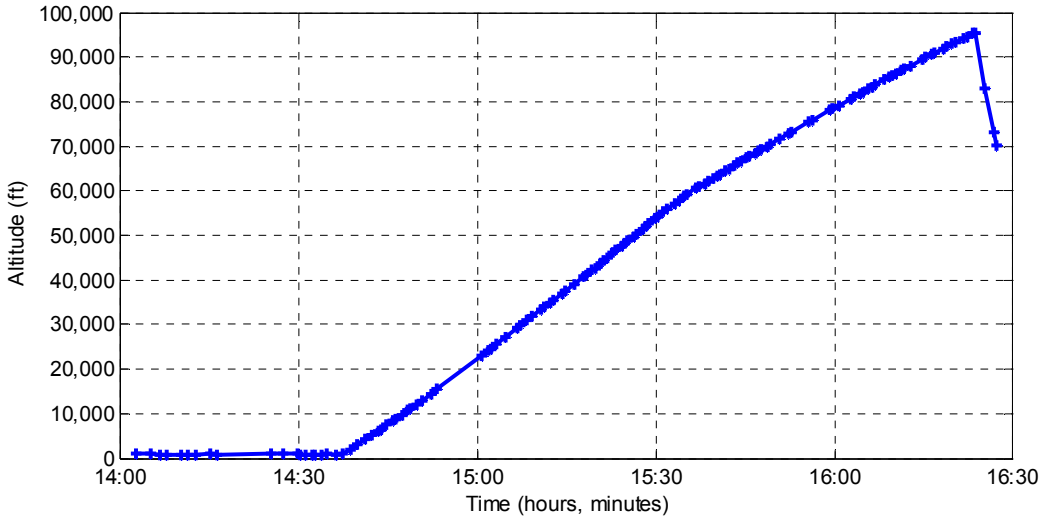

Figure A-5: HABS 16b Altitude Profile

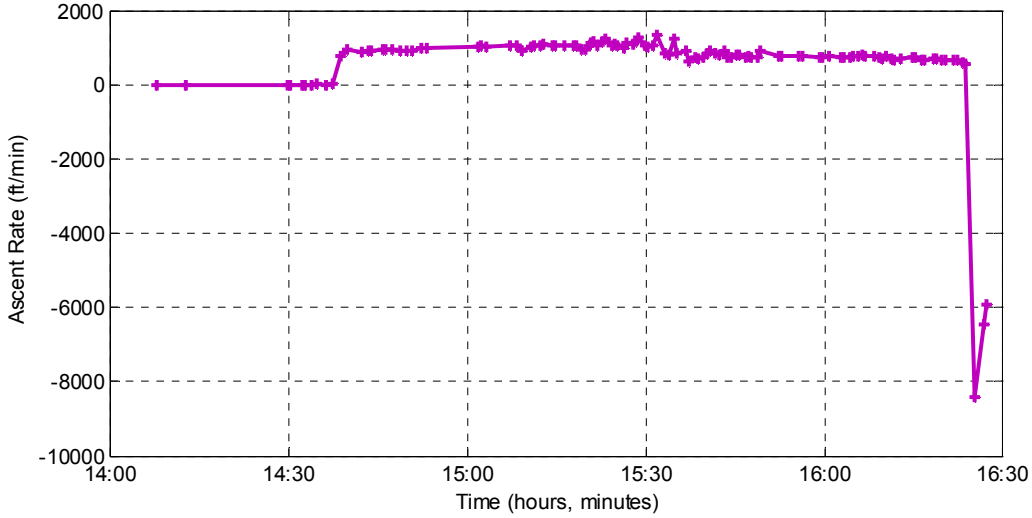

Figure A-6: HABS 16b Ascent Rate

Data from the telemetry log is available in data files on the DVD-ROM.

Appendix B.

Flight Test Dance Cards

Mars UAV Demonstrator	Flight: 1	Date:
Card: 1 Line-Up		
Prelim		
	Checked by:	
Flight Test Director: _____ HABS Launch Director: _____ HABS Ground Station Operator: _____ UAV Ground Station Operators 1 & 2: _____ _____ Chase 1 Lead: _____ Chase 2 Lead: _____ Chase 3 Lead: _____		
	Time:	1

Mars UAV Demonstrator	Flight: 1	Date:
Card: 2 Mission Limits		
Prelim		
	Checked by:	
General Weather Conditions: Wind Speed: _____ Wind Direction: _____ Predicted HABS Landing Point (lat/lon): _____ _____ Predicted UAV Landing Point (lat/lon): _____ _____		
	Time:	2

Mars UAV Demonstrator		Flight: 1	Date:
Card: 3 Preflight Tests			
Prelim			
		Checked by:	
A	Battery Checks		
B	HABS System On		
C	UAV Avionics On		
D	HABS Telemetry Check		
E	UAV Telemetry Check		
F	GPS Lock		
G	UAV IMU Calibration		
	Time:		3

Mars UAV Demonstrator	Flight: 1	Date:
Card: 4 Balloon Prep / Chase 1		
Ascent		
	Checked by:	

A	Prepare HABS Parachute	
B	LiftWin Calculations Required Lifting Force:	
C	Move to Launch Site Time: _____	
D	Fill Balloon Measured Lifting Force: _____	
E	Stage Payloads for Launch	
F	Chase 1 Departs toward Predicted Landing Point	
	Time:	4

Mars UAV Demonstrator	Flight: 1	Date:
Card: 5 Balloon Launch		
Ascent		
	Checked by:	

A	Release Balloon to Tethers	
B	Countdown	
C	Release Time: _____	
D	Update Landing Point Predictions	
E	Advise Chase 1 of Launch Time and Updated Predictions	
	Time:	5

Mars UAV Demonstrator	Flight: 1	Date:
Card: 6 Chase 2 & 3		
Ascent		
	Checked by:	

A	Chase 2 Departs for Landing Point	
B	Chase 3 Departs for Landing Point	
C	Monitor Balloon Telemetry	
D	Compare Trajectory with Prediction	
E	Advise Chase Teams of Updates as Necessary	
	Time:	6

Mars UAV Demonstrator		Flight: 1	Date:
Card: 7 Drop / Pull-Up			
Cut-Down			
		Checked by:	
A	At Press. Alt. 116,000 ft: UAV Motor On Release from Balloon/HABS		
B	UAV Pull-Up		
C	Level Cruise 120 knots (200 ft/s)		
D	HABS Release from Balloon (or balloon burst)		
	Time:		7

Mars UAV Demonstrator	Flight: 1	Date:
Card: 8 Test Maneuvers		
Test Maneuvers		
	Checked by:	

A	RAP Commands Pitch Roll Yaw	
B	Doublets Pitch Roll Yaw	
C	Repeat Doublets Pitch Roll Yaw	
D	(Optional) Pitch Frequency Sweep	
E	Repeat Test Maneuver Sequence until Motor Battery Depleted 110,000 ft / 120 KCAS	
	Time:	8

Mars UAV Demonstrator	Flight: 1	Date:
Card: 9 Begin Descent		
Descent		
	Checked by:	

A	Begin UAV Descent, 1000 ft/min	
B	Navigate UAV to Predicted Landing Point	
C	Reduce Telemetry Data Rate	
	Time:	11

Mars UAV Demonstrator	Flight: 1	Date:
Card: 10 Parachute Deploy		
Descent		
	Checked by:	

A	Trigger UAV Parachute above 60,000 ft or 60 minutes after descent began	
	Time:	12

Mars UAV Demonstrator	Flight: 1	Date:
Card: 11 Track / Recover		
Recovery		
	Checked by:	

A	Chase 1, 2, 3 Assigned to Track UAV or HABS by Flight Test Director	
B	Monitor Telemetry	
C	Update Predicted Landing Points	
D	Repeat Until UAV and HABS are Located	
E	Turn Off Electronics upon Finding HABS and UAV	
F	Return to Base	
G	All Payloads Shall Remain Sealed until Returned to Base for Inspection	
	Time:	13

Appendix C.

Supplemental DVD-ROM Contents

Computer files containing test data and multimedia related to this thesis are available in DVD-ROM format from the author. Copies of this document are located in the root folder of the disc.

Defense Slides - This folder contains the slideshow and movie clip presented on 30 July 2007 at the oral defense of this thesis.

HABS - This folder contains data and images from the high altitude balloon launches conducted by the Experimental Balloon Society in support of this research. This folder contains subfolders containing files particular to specific flights.

HABS 15 - This folder contains images and data from the HABS 15 flight on 10 March 2007.

Telemetry Comparison - This folder contains maps created from telemetry data recorded by the HABS and the MNAV avionics unit on 10 March 2007. These files were created for use with Google Earth software.

Temperature Data - This folder contains the temperature data recorded on the 10 March 2007 balloon flight.

HABS 16b Photos - This folder contains images of the 28 April launch of a high altitude

balloon carrying a mock-up of a UAV and its avionics and telemetry system.

Images - This folder contains images related to the research presented in this thesis. Miscellaneous images reside at this level, but other images are collected in subfolders.

APEX Simulation - This folder contains images related to NASA Dryden's APEX program.

ARF Modifications for Mars Airplane Project - This folder contains images documenting the modifications made to the Almost-Ready-to-Fly model sailplane kit.

ARF's First Flight - This folder contains images of the low altitude UAV used as an avionics testbed. The images show the aircraft just before takeoff, during the flight, and after recovery.

Helicopter Moments of Inertia Tests - The images in this folder demonstrate the use of the three-string pendulum system for measuring the moments of inertia of a small UAV. This method is described in Section 4.1.

KU Mars Airplane Demonstrator AE721 - This folder contains the slideshow from the Final Design Review presentation of the Mars UAV project at the University of Kansas in Fall 2006 semester. The slideshow describes the design of a high altitude demonstrator UAV.

Misc - This folder contains miscellaneous data files related to this research, such as the

contour points of the E206 Airfoil.

NASA Movies - This folder contains clips of the NASA high altitude UAV called ARES. Also, two animations of flight over the Mars surface are included.

Sources - This folder contains most of the articles cited in this thesis in Adobe PDF format. Additional articles are also included that are tangentially related to this thesis and may be useful for future research.

Appendix D.

Bird of Time Model Sailplane Drawings